iScience

CellPress

Article

Zebrafish Exploit Visual Cues and Geometric Relationships to Form a Spatial Memory

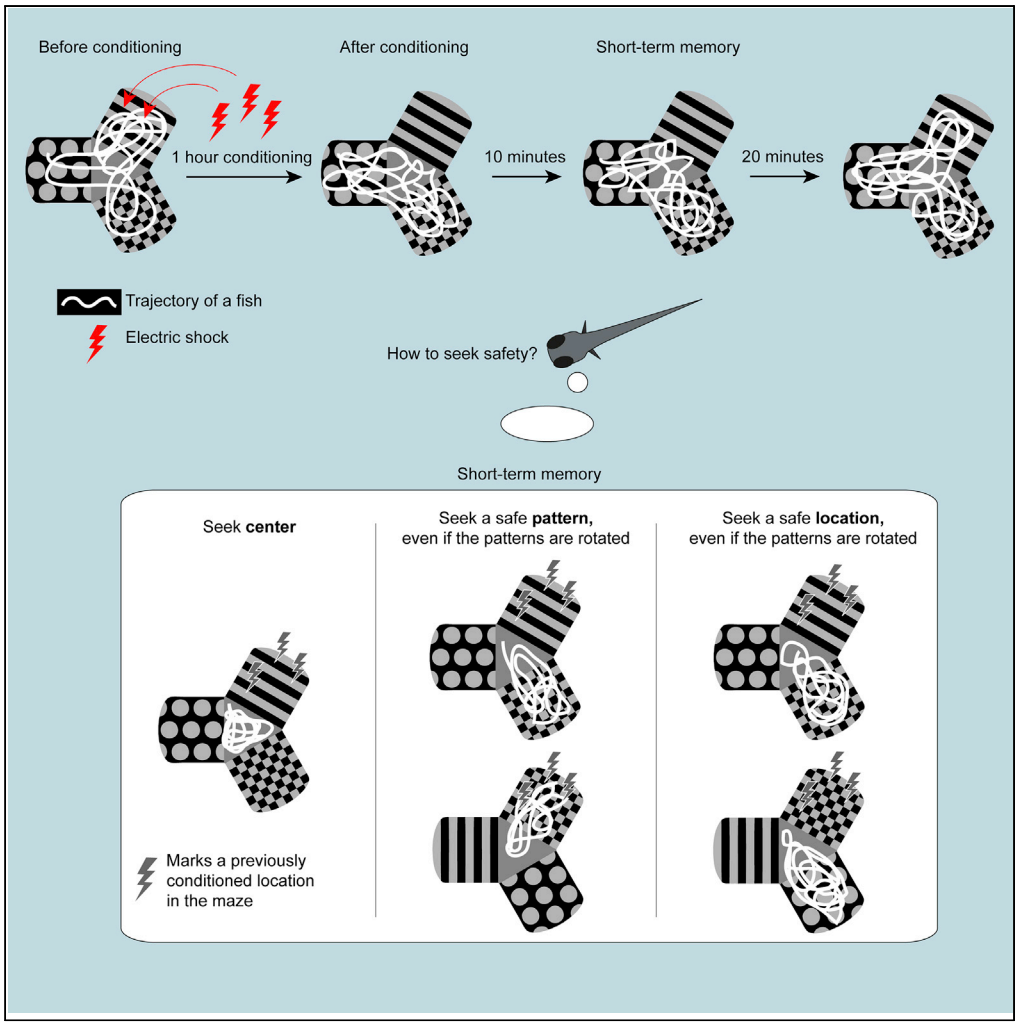

Ksenia Yashina, Álvaro Tejero-Cantero, Andreas Herz, Herwig Baier

hbaier@neuro.mpg.de

HIGHLIGHTS

Zebrafish as young as 3 weeks learn to avoid one arm of a Y-maze within an hour

The memory depends on the presence of visual cues and lasts for at least 10 min

Fish use various safety seeking strategies: prefer the center, one or two safe arms

Safety can be associated with a visual cue or with a location in the maze

Yashina et al., iScience 19, 119–134
September 27, 2019
https://doi.org/10.1016/j.isci.2019.07.013

iScience

CellPress

Article

Zebrafish Exploit Visual Cues and Geometric Relationships to Form a Spatial Memory

Ksenia Yashina,[1,2] Álvaro Tejero-Cantero,[3,4] Andreas Herz,[2,3,4] and Herwig Baier[1,2,5,*]

SUMMARY

Animals use salient cues to navigate in their environment, but their specific cognitive strategies are largely unknown. We developed a conditioned place avoidance paradigm to discover whether and how zebrafish form spatial memories. In less than an hour, juvenile zebrafish, as young as 3 weeks, learned to avoid the arm of a Y-maze that was cued with a mild electric shock. Interestingly, individual fish solved this task in different ways: by staying in the safe center of the maze or by preference for one, or both, of the safe arms. In experiments in which the learned patterns were swapped, rotated, or replaced, the animals could transfer the association of safety to a different arm or to a different pattern using either visual cues or location as the conditioned stimulus. These findings show that juvenile zebrafish exhibit several complementary spatial learning modes, which generate a flexible repertoire of behavioral strategies.

INTRODUCTION

When performing a behaviorally relevant task, such as seeking a refuge or a feeding spot, animals rely on various environmental cues to memorize and recall specific locations (Cheng, 1986; Durán et al., 2010; Eichenbaum, 2017; Franz and Mallot, 2000; Gouteux et al., 2001; Kelly et al., 1998; Salas et al., 2006; Vallortigara et al., 1990). Teleost species, such as adult goldfish, have been shown to use several strategies to navigate in diverse locales and may associate a reward with specific places, with geometric configurations of the environment, or with local visual cues (López et al., 2000, 1999; Vargas et al., 2004). The reward can also be associated with a combination of these cues, e.g., with the animal's location in a plus-shaped maze and a salient visual stimulus. When the visual cue is relocated, the cue-guided strategy becomes incompatible with a location-guided strategy, and the fish may choose one of the two strategies. Surprisingly, some fish choose a strategy of following the visual cue, whereas others use a strategy of seeking the location (López et al., 2000).

Few studies have addressed the question of spatial learning strategies in zebrafish, a genetically tractable model organism. Adult zebrafish are capable of associative learning using, among others, visual, olfactory, and geometric cues (Al-Imari and Gerlai, 2008; Aoki et al., 2015; Braubach et al., 2009; Kalueff et al., 2013; Kenney et al., 2017; Lal et al., 2018; Lee et al., 2012, 2013, 2015; Sison and Gerlai, 2010). Much less is known about the learning abilities of larval and juvenile zebrafish before the age of 4 weeks, a period during which the brain is accessible to non-invasive imaging approaches. There have been reports of learning effects in 1-week-old larval zebrafish using classical conditioning paradigms (Aizenberg and Schuman, 2011; Harmon et al., 2017; Lee et al., 2010) and operant conditioning paradigms (Hinz et al., 2013; Yang et al., 2019). Robust learning effects were observed in 3-week-old juvenile zebrafish (Matsuda et al., 2017; Valente et al., 2012). Although these studies demonstrated the ability of zebrafish to associate cues with a reward or a punishment, spatial components of learning are mostly unexplored.

To investigate the mechanisms underlying the flexibility in selecting specific navigation strategies, we developed a Y-maze paradigm. Here, fish were conditioned to avoid one of three arms of the Y-maze by cueing one arm with electric shocks. This experimental setup allows fish to explore several compartments of the maze in an operant mode while offering the experimenter full control of the fish's visual environment. We characterized the learning behavior of zebrafish in the Y-maze and found robust learning effects in juvenile animals older than 3 weeks. Experiments in which we replaced, swapped, or rotated the visual patterns showed that the animals used a variety of strategies to memorize the safe areas in the maze. Some fish avoided both the conditioned arm and all other arms by staying in the center of

[1]Max Planck Institute of Neurobiology, Martinsried 82152, Germany

[2]Graduate School of Systemic Neurosciences, Martinsried 82152, Germany

[3]Faculty of Biology, Ludwig Maximilians University, Martinsried 82152, Germany

[4]Bernstein Center for Computational Neuroscience, Martinsried 82152, Germany

[5]Lead Contact

*Correspondence: hbaier@neuro.mpg.de

https://doi.org/10.1016/j.isci.2019.07.013

the maze, whereas others preferred either a safe pattern or a safe location in the maze. These findings indicate that zebrafish use visual cues, in conjunction with geometric relationships, to navigate through their environment.

RESULTS

Operant Conditioning in a Y-Maze as a Readout of Spatial Memory

We configured a conditioned place avoidance (CPA) paradigm, in which young zebrafish could explore a Y-maze. Each arm of the maze had a distinct visual pattern associated with it projected from below (Figure 1A). Experiments consisted of three consecutive sessions. In the first session (habituation) fish were free to explore the maze. At the end of this session we identified the arm with the highest occupancy as the preferred arm of each fish, which was then selected as the arm for conditioning. During the second session (conditioning) we trained the fish to avoid the conditioned arm by punishing entry into that arm with a mild electric shock. In the third session (test) the electric stimulation was switched off and the memory of the fish was tested.

We developed two measures to estimate the effects of conditioning (Figure 1B). Our first measure was the occupancy (OC) of each arm, or center of the maze, which we calculated as the proportion of the total experiment time the fish spent in the respective part of the maze. Our second measure was the entry frequency (EF) of each arm, calculated as the number of entries into the respective arm divided by the total number of arm entries. We did not calculate EF measure for the center of the maze, because it was equal to the sum of all arm entries and did not reflect avoidance/preference of maze arms. Using the OC measure, we checked if fish had any intrinsic preference for the visual patterns used in the experiments. We ran control experiments, in which the fish were allowed to swim in the maze for 2 hours without electrical stimulation. The fish did not show a preference for any of the visual patterns (Figure 1D).

For each measure (EF or OC) we created an associated score to evaluate the difference in avoidance/preference of the maze arms (the center of the maze was not included). The score was calculated by subtracting the average of the measures in the two safe arms from the measure in the conditioned arm (Figure 1B, see schematic equation). This score is positive when a fish prefers the conditioned arm and negative when the fish avoids it. We evaluated the stability of the OC and EF scores in the control experiments. The OC and EF scores of the arm that were preferred in the first 30 min of the experiment stayed positive on average over the duration of the control experiment (Figure 1C, see Table S1 for details about the animals used in this and following experiments). This suggests that the arm preference is stable and any change in CPA measures in conditioning experiments is a result of conditioning and not of stochastic variation in the fish's arm preferences.

A Biologically Realistic Agent Model Replicates Learned Avoidance Behavior

Larval and juvenile zebrafish swim in characteristic swim bouts (Video S1). Electric stimulation caused swim bouts of increased amplitude compared with the amplitude of spontaneous swim bouts (Figure 1E). We hypothesized that increased swimming speeds under electric stimulation in the conditioned arm could lead to changes in the OC and EF measures independent of the learning abilities of the fish. We developed a null-model of the CPA measures in the conditions of stimulation-enhanced swim bouts to test our hypothesis (Figure 1F, see Methods). In this computational model, the simulated agent could move in pseudo-random walk fashion in a one-dimensional arm in discrete bouts of size S, with a certain probability of moving into a different arm. The effect of electric shocks on the speed of the fish was simulated by multiplying the bout size in the conditioned arm by a factor $\alpha \geq 1$. Learning was excluded from the design of this basic model. We generated fish trajectories for different values of α and found that the OC score of the conditioned arm, but not its EF score, was dramatically decreased during the conditioning session (Figure 1G, top). This result highlights an effect of increased speed on OC that is independent of learning.

We then added a learning rule to the model by decreasing the probability of entry into the conditioned arm and observed a decrease in both the OC and EF scores of the conditioned arm in conditioning and test sessions (Figure 1G, bottom). We concluded that the decrease in the occupancy of the conditioned arm while the fish is shocked is not sufficient for inferring learning, as it can be explained by learning-unrelated reasons, and decided not to use the OC score during the conditioning phase.

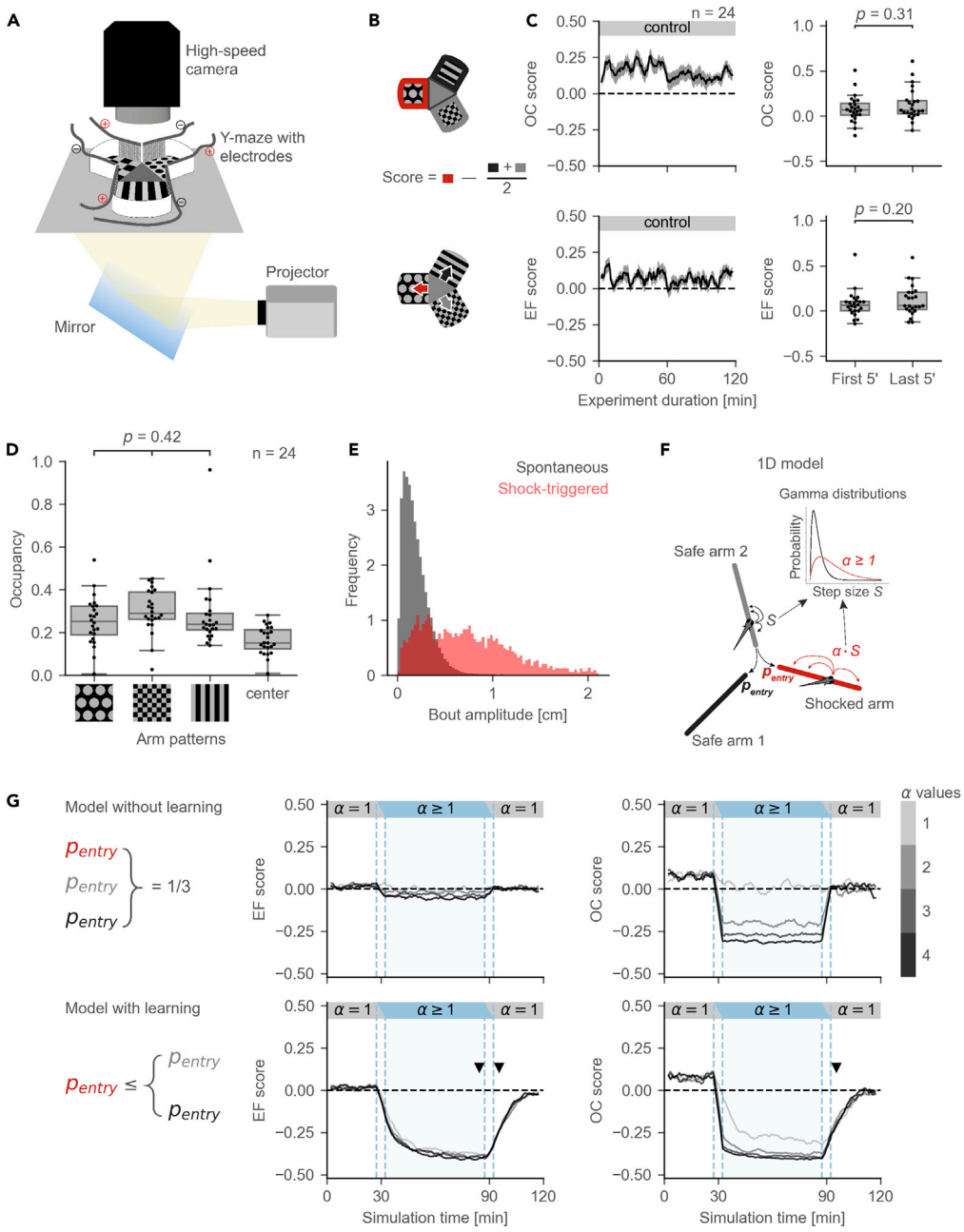

Figure 1. The Conditioned Place Avoidance (CPA) Paradigm

(A) Experimental setup.

(B) Measures of fish performance in the paradigm, top: arm occupancy (OC); bottom: arm entry frequency (EF); middle: schematic for the calculation of the preference scores for OC/EF. Positive values of the scores correspond to arm preference; negative values correspond to arm avoidance. Red color represents the shocked arm, black and gray represent the safe arms.

(C) Left: moving averages of the OC/EF scores in a 2-h control experiment (mean ± SEM). Right: box plots for OC/EF scores in the first and the last 5 min of the control experiments (Mann-Whitney test, n = 24 fish). Box plots show median and quartiles; whiskers show 1.5x interquartile range; dots show values for individual fish; prime symbol stands for minutes.

(D) There is no significant preference for any of the visual patterns (ANOVA, n = 24 fish). Box plot annotations are the same as in (C).

(E) Distributions of amplitudes for spontaneous (gray) and shock-triggered swim bouts (red). Age of the fish is between 20 and 27 days post fertilization.

Figure 1. *Continued*

(F) Pseudo-random 1D walk model used to evaluate CPA measures. Bout amplitude S for simulated movement was drawn from a Gamma distribution, amplitude in the conditioned arm was multiplied by a speed ratio α.

(G) Top: model without learning. Bottom: model with learning. Learning rule was implemented by decreasing the probability of entry into the conditioned arm. Middle and right: moving averages of EF and OC scores. Black/gray lines correspond to simulations with different speed ratios α. Dashed vertical blue lines mark the areas where moving average combined information from two sessions. Arrowheads mark the differences in the OC/EF scores between top and bottom. Moving averages are calculated with a 5-min time window and a 30-s time step.

See also Table S1.

Spatial Learning Abilities Emerge at Juvenile Stages

We used the established paradigm to identify the earliest developmental stage at which zebrafish can be conditioned. We chose three age groups, 1-, 2-, and 3-week-old fish, and performed experiments that consisted of two sessions: habituation and conditioning (Figure 2A). We found that fish had an EF score significantly lower than zero at the end of conditioning only once they reached 3 weeks of age (Figure 2B). The OC score was significantly decreased in all age groups at the end of conditioning; however, this result was predicted by our computational model and could be unrelated to the learning ability of the animals (Figure 2C). The size of the fish was larger at later stages of development (Figure 2D). Based on this comparison of different age groups we selected fish older than 3 weeks for further experiments.

Memory of Visually Cued Place Persists for at Least Ten Minutes

We tested the duration of the aversive memory formed at the end of conditioning in the third (test) session of the protocol, during which electric shocks were switched off (Figure 3A). Analysis of the OC score revealed that fish had formed a memory of the aversive arm: the OC score was below zero in the first 10 min of the test session (Figure 3A, permutation test p value = $7 \cdot 10^{-4}$, n = 40 fish). At the end of the test session the OC score returned to zero (Figure 3A, permutation test p value = 0.21, n = 40 fish).

To investigate how robust the formed memory was, we introduced a no-pattern session into the experimental protocol between the conditioning and test sessions: after the conditioning session, electric stimulation was switched off and all patterns were switched to a gray background for 5 min (Figure 3B). During this featureless session, avoidance of the conditioned arm was abolished: the OC score was not significantly different from zero (Figure 3B, permutation test p value = 0.48, n = 30 fish). However, the fish continued to avoid the conditioned arm after the visual patterns were shown again at their original locations (Figure 3B, permutation test p value = $7 \cdot 10^{-3}$, n = 30 fish). This finding suggests that the fish use visual cues to retrieve an association between a specific place and the aversive stimulus. To rule out alternative mechanisms, such as odor cues left by the fish after being shocked, we used a Y-maze with three identical patterns (Figure 3C). The occupancy of the conditioned arm was significantly reduced during the conditioning session (Figure 3C, permutation test p value = 10^{-4}, n = 31 fish), as predicted by our computational model (Figures 1F and 1G). However, there was no significant avoidance of the conditioned arm in the test session (Figure 3C, permutation test p value = 0.09, n = 31 fish). This result suggests that, in this experimental setup, fish rely on visual cues and not on outside landmarks or on in-maze cues, such as odors, or other sensory modalities, to both retrieve and form an associative memory.

An analysis of EF scores in these three experiments revealed similar effects (Figure S1). Combined, these results suggest that the memory of the conditioned arm persists for at least 10 min after the end of conditioning and that it depends on the presence of visual cues.

Orientation within the Electric Field Predicts Strength of Response and Success of Conditioning

We observed a strong variability in individual responses to electric shocks (see the spread of bout amplitudes in Figure 1E, red histogram) and investigated the potential causes behind it. It has previously been reported that fish respond to electric shocks more strongly when oriented parallel to the electric field (Tabor et al., 2014). We confirmed that the probability of response is higher when the fish is aligned with the electric field (Figures 4A and 4B). Moreover, the strength of the response is significantly higher when the fish is oriented toward the cathode than toward the anode (Figure 4C).

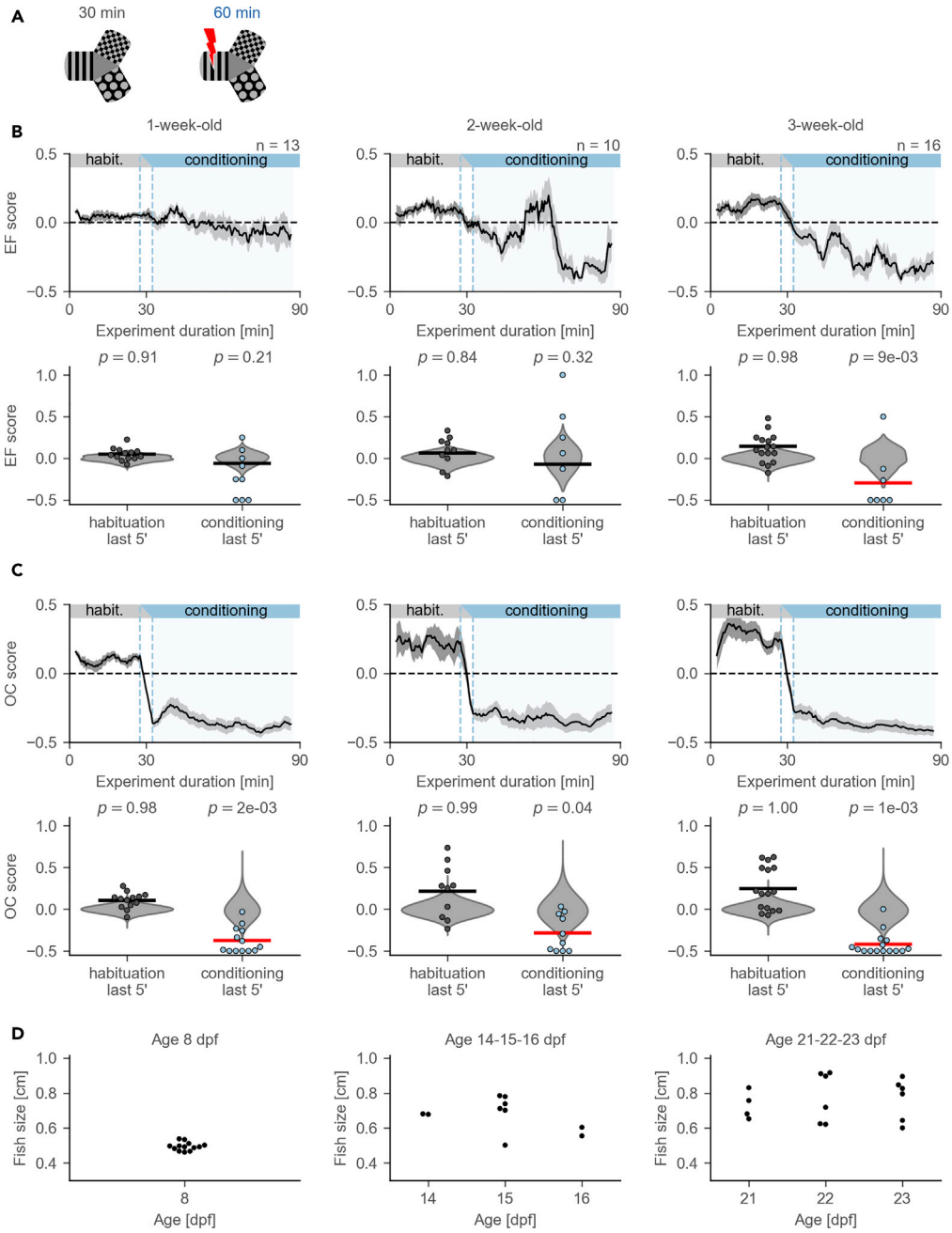

Figure 2. Performance in the CPA Paradigm across Different Age Groups

(A) Schematic of the protocol: habituation and conditioning sessions.

(B) Changes in EF scores across different age groups. Note that the EF score becomes significantly lower than zero only in 3-week-old fish. Top: moving average (mean ± SEM). Bottom: comparison of the EF scores in the last 5 min of conditioning with the null-distribution (permutation test). Individual values for each fish are shown as dots; null-distributions are shown in gray violin plots. Horizontal lines show the sample means; the line is red if the mean lies to the left of the fifth percentile in the null-distribution. Prime symbol stands for minutes.

(C) Changes in OC scores across different age groups. Figure annotations are the same as in (B).

(D) Distribution of body sizes across different ages. Average body size and its variability increase with age: 1 week, 4.95 ± 0.23 mm; 2 weeks, 6.74 ± 0.93 mm; 3 weeks, 7.64 ± 1.15 mm, mean ± standard deviation. Dpf, days post fertilization.

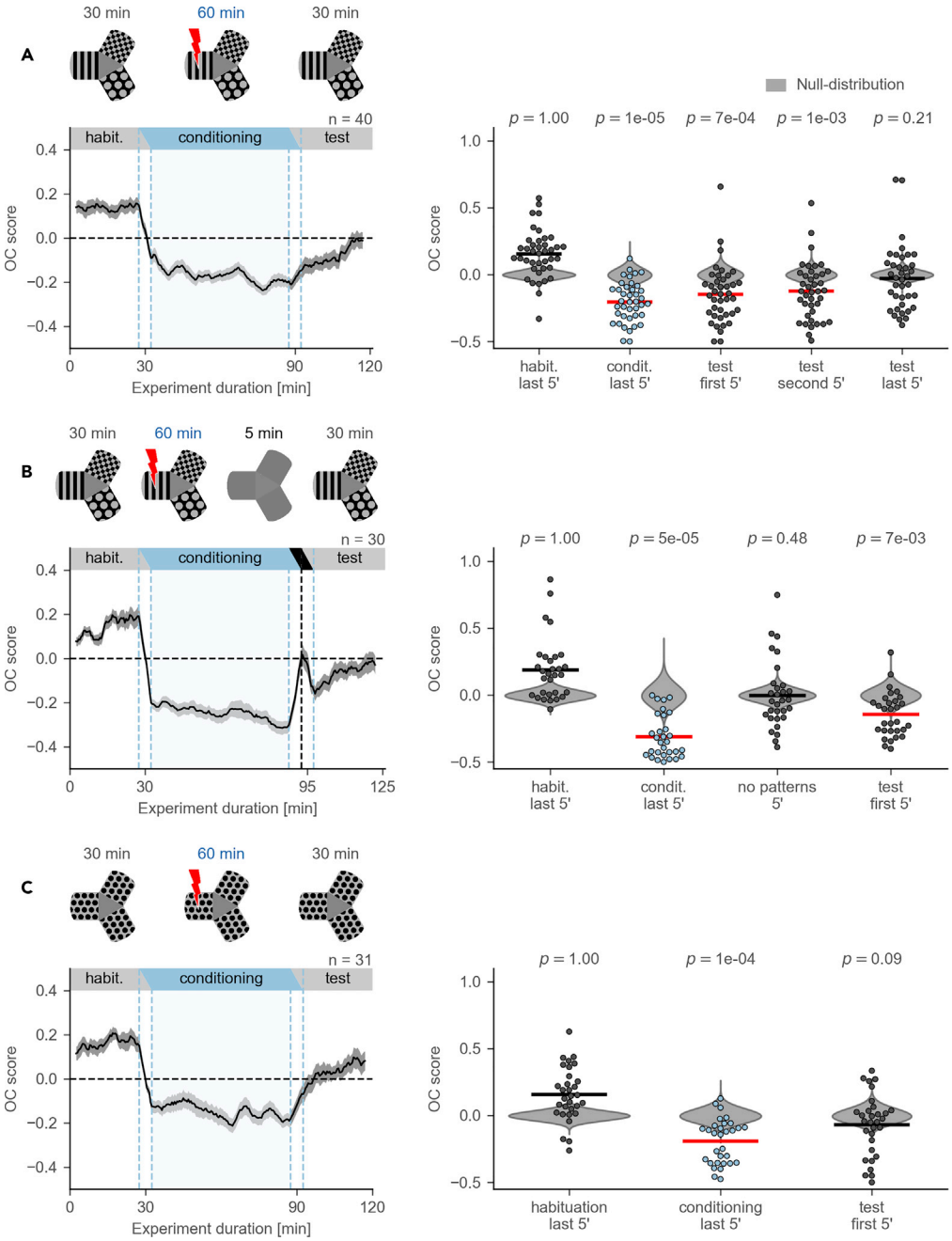

Figure 3. Evaluation of Aversive Memory Formed in the CPA Paradigm

(A) Top: schematic of the protocol with habituation, conditioning, and test sessions. Bottom, left: OC score moving average. Black line shows average across individuals, gray ribbon shows SEM. Bottom, right: comparison of the OC scores in the last 5 min of conditioning and in the first, second, and last 5 min of test session with the null-distribution (permutation test, n = 40 fish). Prime symbol indicates minutes.

(B) Top: schematic of the protocol with habituation, conditioning, no-pattern (all arms with a gray background), and test sessions. Bottom, left: OC score moving average. No-pattern session is indicated on the top of the plot with a black horizontal bar. Note the deflection in the moving average during the no-pattern session (at around minute 95) with a peak value near zero, the chance level. Bottom, right: comparison of the OC scores in the last 5 min of conditioning, 5 min of no-pattern, and in the first 5 min of test session with the null-distribution (permutation test, n = 30 fish).

Figure 3. *Continued*

(C) Top: schematic of the protocol where visual patterns in all arms are identical. Bottom, left: OC score moving average. Bottom, right: comparison of the OC scores in the last 5 min of conditioning and in the first 5 min of test session with the null-distribution (permutation test, n = 31 fish). All moving averages are calculated with a 5-min time window and a 30-s time step.

See also Figure S1.

To reveal any structure in the amplitudes and onset times of the responses, we plotted all individual responses to electric shocks as speed curves in one graph (Figure 4D). Hierarchical clustering with Ward's linkage method showed three distinct clusters of response types (Figure 4E). The two low-amplitude (LA) response types differed primarily in their onset time. Moreover, they occurred when fish were in opposing orientations: early-onset LA responses occurred mostly in the anode-facing orientation; late-onset LA responses tended to occur in the cathode-facing orientation. The third group, high amplitude (HA) responses, occurred predominantly when fish were in the cathode-facing orientation.

We hypothesized that different response types correlate with the perceived strength of the shocks and thus with avoidance level of the conditioned arm. Avoidance level could be quantified by calculating the OC and EF scores in the 5-min interval immediately after the occurrence of each individual shock response, which we grouped by the response type. The OC and EF scores turned out to be significantly lower after the HA response type than after either early- or late-onset LA responses (Figure 4F). The reduction in OC score could be explained by the effects of electric shocks (see Figure 1G), whereas the lower EF score shows that the occurrence of HA responses correlated with stronger learned avoidance of the conditioned arm.

Spatial Learning Strategies Differ among Individual Fish

To investigate how avoidance strategies are implemented by individual fish, we grouped their trajectories in the maze in the last 5 min of conditioning (see Methods). Each individual trajectory could be described by the occupancies of the three arms and the center. We visualized these occupancies of each animal using a color code (Figure 5A). We used hierarchical clustering on the occupancies and identified three main groups of trajectories: fish preferring the central compartment of the maze to all three arms (4 fish), fish that did not avoid the conditioned arm (9 fish), and fish that avoided the conditioned arm by preferring to stay in one or two safe arms (27 fish) (Figure 5A). We did not observe systematic size differences between fish with different strategies (fish body length, mean $\pm$ SD: center-preferring 9.8 $\pm$ 0.9 mm, non-avoiding 10.5 $\pm$ 1.6 mm, avoiding 10.1 $\pm$ 1.0 mm, ANOVA p value = 0.63, F = 0.47). When we compared the swimming trajectories of individual fish in the last 5 min of conditioning and in the first 5 min of the test session, we found that they were stable for the majority of the fish (Figure 5B, see individual examples in Figure 5C). This indicates that individual fish choose a persistent navigational strategy, at least as long as the visual cues are stable.

Fish May Form a "Map of Safety" of the Y-Maze

We hypothesized that manipulation of the visual cues could reveal which cues are relevant for the fish to navigate in the maze. First, we tested the hypothesis that the fish use a pattern aversion strategy to avoid the conditioned arm. We performed experiments with a new cohort of fish, in which, after conditioning, we replaced the conditioned pattern with a new visual pattern in the same arm (Figures 5D and 5E, see schematic). Three groups of swimming patterns were observed in this cohort of fish, with center-preferring fish (5 fish), fish not avoiding the conditioned arm (9 fish), and fish avoiding the conditioned arm (20 fish). Interestingly, fish continued to avoid the conditioned arm even after the conditioned pattern was replaced (Figure 5E, blue left column indicates avoidance; see also Figure S2). Individual trajectories illustrate how fish continue to avoid the conditioned arm (Figure 5F). Control experiments with pattern replacement without conditioning confirmed that replacing one pattern was neither intrinsically aversive nor attractive to the fish (Figure S3). These results suggest that fish may not only learn to avoid a visual pattern but also form a "map of safety," which influences their navigational behavior in the Y-maze.

Next, we tested the hypothesis that the fish learn to prefer a safe pattern. We performed experiments in which two safe patterns were swapped after conditioning (Figures 6A and 6B, see schematic). In these experiments, we identified two groups of center-preferring (4 fish) and safe-arm-preferring individuals (28 fish) (Figure 6A). The analysis of the OC/EF scores showed that the fish successfully avoided the conditioned arm even after the safe patterns were swapped, i.e., the fish retained their aversive memory of the

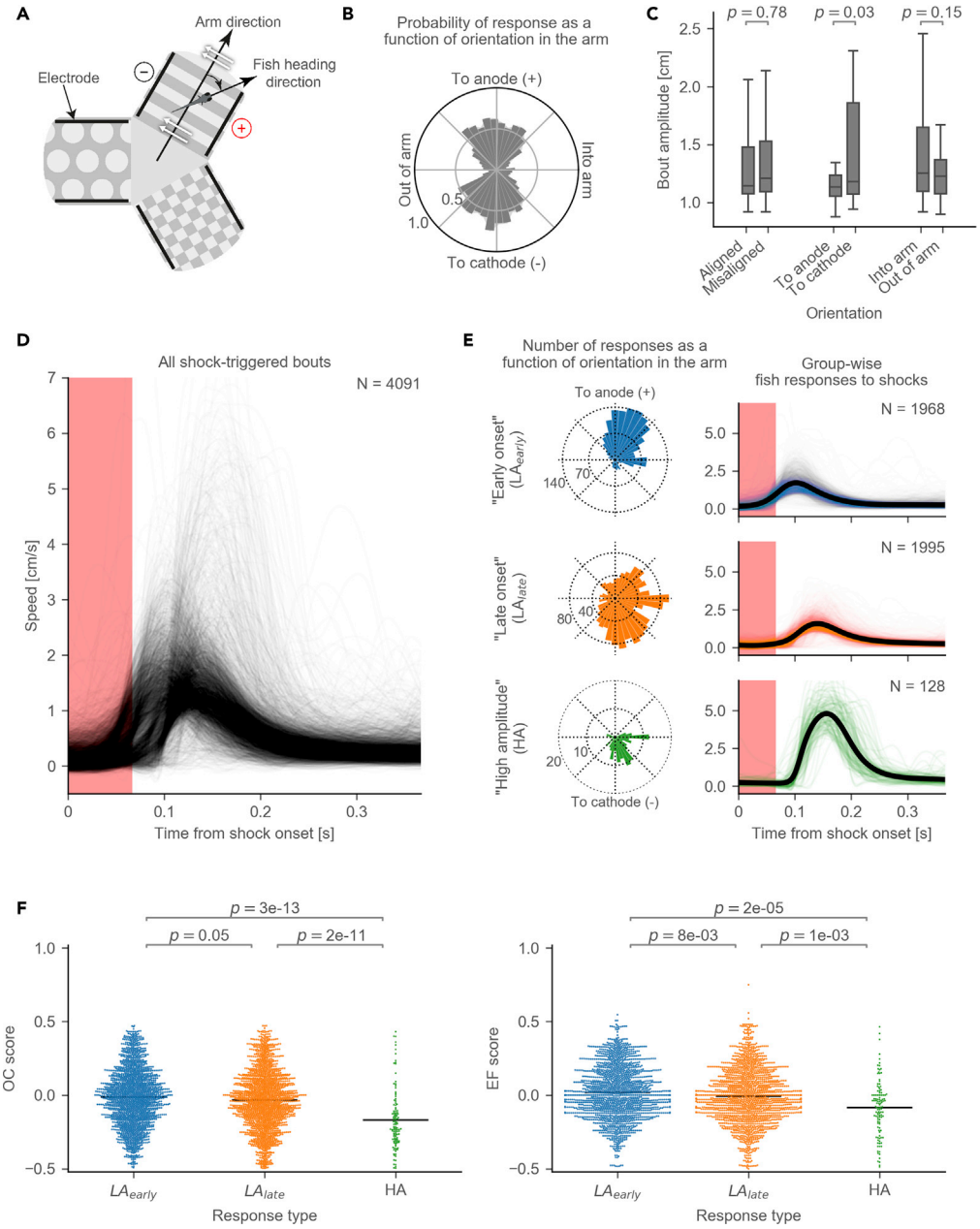

Figure 4. Responsiveness to Electric Shocks

(A) Schematic of a fish's orientation in the electric field. The orientation angle is calculated between arm direction and fish heading direction. White arrows show the direction of the electric field. Black lines indicate the positions of the electrodes.

(B) A radial histogram of the probabilities of shock-triggered swim bouts (i.e., responses to shocks) plotted against the fish's orientation in the electric field (bin size 9°).

(C) Comparison of the bout amplitudes between different orientations in the electric field (2-sample t test). Bout amplitude is calculated as speed integrated over the duration of a bout. "Aligned" bouts include anode- and cathode-facing orientations; "misaligned" bouts include into-arm- and out-of-arm-facing orientations.

(D) Variety of amplitudes and onsets of individual shock-triggered swim bouts. Each curve shows the speed during an individual bout (N = 4,091 bouts).

(E) Response types identified by hierarchical cluster analysis: low amplitude with early onset (LA_{early}, N = 1,968 bouts), low amplitude with late onset (LA_{late}, N = 1,995 bouts), and high-amplitude responses (HA, N = 128 bouts). Left: radial

Figure 4. *Continued*
histogram of how many bouts of a certain type occur plotted against the fish's orientation in the electric field (bin size 9°). Right: speed over time after the shock onset. Y axes are the same as in (D).
(F) Comparison of OC (left) and EF (right) scores in a 5-min time window after a shock-triggered bout between different response types (Mann-Whitney test). Each dot represents an OC or EF score after an individual shock-triggered bout. Horizontal lines indicate sample means. Bouts were obtained from the experiments with 27 fish.

conditioned arm (Figure 6B, blue left column indicates avoidance; see also Figure S4). After swapping the two safe patterns, we observed two different behaviors. About two-thirds of the animals "followed the pattern" and switched their preference to another safe arm, i.e., these fish stayed with the preferred visual pattern (Figure 6B, red in the right column). The other third continued to prefer the same arm despite the pattern swap, i.e., these fish kept the preferred location (Figure 6B, red in the middle column). Individual trajectories illustrate these two different strategies (Figure 6C). This result suggests that fish can use location, rather than rely solely on visual information, in the Y-maze to seek safety.

Finally, we tested the strength of the safety-seeking behavior by creating a conflict between safety and avoidance cues. We rotated the visual patterns after conditioning such that the conditioned pattern was moved into the preferred safe arm (Figures 6D and 6E, see schematic). In the test session, we found that some fish continued to swim in their preferred arm despite the presence of the conditioned pattern (Figure 6E, red in the left column; Figure 6F). Other fish transferred their preference according to the pattern rotation, i.e., these fish started to avoid the previously preferred arm (Figure 6E, red in the right column; Figure 6F). In summary, we observed that individual fish learn to associate safety either with (one or more) visual patterns or with location in the maze.

DISCUSSION

To determine whether juvenile zebrafish are capable of spatial learning, we devised CPA in a Y-maze as a new behavioral paradigm. In our setup, swimming into one of the three arms is punished with a mild electrical shock, and most of the fish learn to avoid this arm within an hour of conditioning. The behavioral chamber is cued with a floor of visual patterns, which can be altered in any desired fashion. The shape of the Y-maze allows for a straightforward readout of the animal's preferred location, i.e., the three arms or the central, uniformly gray compartment. Manipulation of the sensory environment in the maze, via replacement, swapping, or rotation of visual patterns, revealed that individual fish use different learning strategies to solve the problem.

Zebrafish older than 3 weeks show robust responses to conditioning in the CPA paradigm, whereas larvae at 1 week post fertilization fail to learn the association, in agreement with previous observations (Valente et al., 2012). Two-week-old zebrafish show highly variable responses. A possible explanation for this variability is that fish at that age differ strongly in their developmental stage, as is suggested by their widely varying body length (see Figure 2). If brain development correlates with body length, then fish siblings may show different learning capacities depending on their size. This observation can be used in future experiments to select groups of fish based on their developmental maturity rather than chronological age.

The effects of conditioning were assessed with two measures: arm occupancy (OC) and arm entry frequency (EF). Although these measures are often correlated (the more frequently the fish enters an arm, the higher the occupancy of that arm, at least if all other motion parameters stay fixed), we demonstrated that they can also decouple because of mechanisms unrelated to learning. A computational model showed that a lowered occupancy of the conditioned arm during conditioning can be explained by the fish's reaction to electric shocks (i.e., by increased speed of swim bouts in the conditioned arm) even when no learning is taking place. Thus, a drop in the OC score is not a reliable indicator of learning in the presence of electrical shocks (i.e., during the conditioning phase). However, a reduced OC score without electrical shocks (i.e., during the test phase) can be explained only by memory of previous punishment. At the same time, the second measure, the entry frequency of the conditioned arm, is not affected by increased swim speed. These results are consistent with the performance of the young larvae, who do not learn in the CPA paradigm: their occupancy measure decreases during training, but their entry frequency is unaltered.

In juveniles, both OC and EF measures of the conditioned arm decrease during conditioning and persist at a reduced value for at least 10 min after cessation of the shocks. The memory is robust to a brief removal of

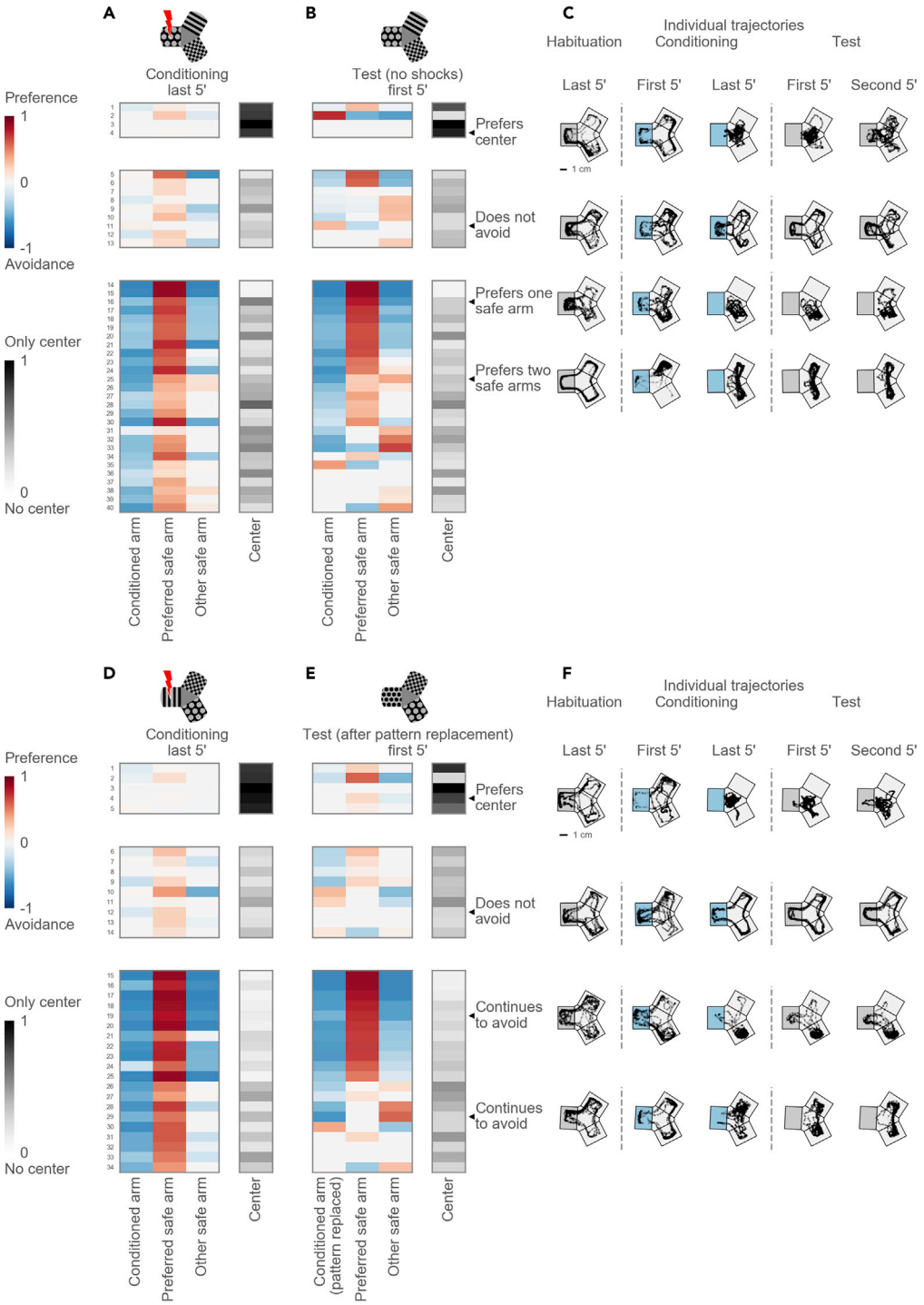

Figure 5. Diverse Strategies Used to Avoid the Conditioned Arm

(A) Top: schematic of the maze during the conditioning session. Bottom: hierarchical clustering of arm occupancies in the last 5 min of the conditioning session reveals three groups: 4 fish preferring the center, 9 fish not avoiding the conditioned arm, and 27 avoiding fish. Each group is presented as a table, one row per fish. Columns correspond to maze arms (from left to right: the conditioned arm, the preferred safe arm, the other safe arm) and the center. Each cell shows a color-coded occupancy value in the particular compartment of the maze for a particular fish, with the logarithmic blue-to-red color scheme for the maze arms and the gray color scheme for the maze center.

Figure 5. *Continued*

(B) Top: schematic of the maze during the test session. The rows in (A) and (B) correspond to the same fish. Rows within each group are ordered by their similarity to each other in the hierarchical tree in the test session.

(C) Example trajectories of individual fish in the last 5 min of habituation, in the first and last 5 min of conditioning, and in the first and second 5 min of test session. Top: a fish uses the central compartment as a "safe haven." Upper middle: a non-avoiding fish revisits the conditioned arm despite continued shocks. Lower middle: a fish prefers one safe arm. Bottom: a fish swims in both safe arms. The conditioned arm is depicted with gray background for the habituation session, blue for the conditioning session, and again gray for the test session. The orientation of the conditioned arm varied in the experiments and is shown here on the left for clarity.

(D) Top: schematic of the maze during the conditioning session in experiments with pattern replacement. Bottom: hierarchical clustering reveals three groups: 5 center-preferring, 9 non-avoiding, and 20 avoiding fish.

(E) Top: schematic of the maze during the test session in experiments with pattern replacement. Bottom: occupancies during the test session that correspond to the groups identified in (D).

(F) Example trajectories of individual fish before and after the pattern replacement. Top: a fish prefers the center. Upper middle: a non-avoiding fish. Lower middle: a fish swims in one safe arm before and after the replacement of the conditioned pattern. Bottom: a fish swims in both safe arms before and after the pattern replacement.

See also Figures S2 and S3.

distinct visual cues between the conditioning and test sessions (see Figure 3). However, the avoidance of the shocked arm diminishes by the end of the 30-min-long test session. Such rapid memory extinction is in contrast with fear conditioning studies in rodents (Fanselow, 1990). Usually, one electric shock is sufficient for a rodent to establish a strong and lasting aversion to a conditioned location. Fish, on the other hand, repeatedly revisit the conditioned arm of the Y-maze. Such behavior can be interpreted as evidence for poor learning. In adult zebrafish, memory formation and retention depend on the telencephalon (Lal et al., 2018). This brain structure may not be fully mature in larval and juvenile zebrafish. Alternatively, rapid memory extinction may serve a different behavioral strategy. Indeed, in the wild, two behavioral drives compete against each other in the fish, the need to avoid danger and the need to forage. In flowing or turbulent water, the positions of objects, predators, and prey change quickly. Such volatility could reward a strategy of returning to a previously dangerous place, given that the threat may be gone and food may have become available in the meantime.

The mechanism behind the gradual loss of conditioned aversion in the test session could be passive, where fish forget, or active, where fish re-learn the safety of the previously conditioned arm. Active re-learning should depend on the presence of the visual cues (given their relevance in the paradigm; see Figure 3C) and should occur when the fish visits the arm with the conditioned pattern and receives no electric shock, thus building a new association of safety with the previously conditioned arm. Passive memory loss should be a function of time and take place independently of the presence of the visual cues. Further experiments, such as memory re-instatement though re-introduction of electric shocks, are necessary for distinguishing between these two processes.

The responsiveness to shocks depends on the orientation of the fish in the electric field, a phenomenon that has been observed previously (Tabor et al., 2014). As a consequence, the electric shocks frequently do not elicit a response when the fish is oriented perpendicular to the electric field. This suggests that such shocks might be ineffective as aversive stimuli. To improve the effectiveness of conditioning, the experiment could be amended in at least two ways. Electric shocks could be applied only when the fish is oriented toward the electrodes (i.e., is aligned with the electric field). Alternatively, more electrodes could be added to the setup so that the fish is always facing them, independent of its orientation.

Analysis of individual responses to electric shocks revealed three response types: two LA types and one HA type. LA response types clearly separate into those correlated with shock onset (early onset) and those correlated with shock offset (late onset). Interestingly, this separation is correlated with the orientation of the fish at the moment of the shock. In particular, early-onset swim bouts occur when the fish is oriented toward the anode, whereas late-onset swim bouts occur in fish facing the cathode. We hypothesize that the polarity of the pulse matters for triggering the response. Briefly, two steel-mesh electrodes, such as those used for shock delivery, could act as plates of a capacitor. The capacitor charges during the electric pulse and discharges after the pulse is switched off, thereby creating a transient current in the opposite direction to the current from the original pulse, hence effectively presenting a pulse in one direction during shock onset and one in the opposite direction during shock offset.

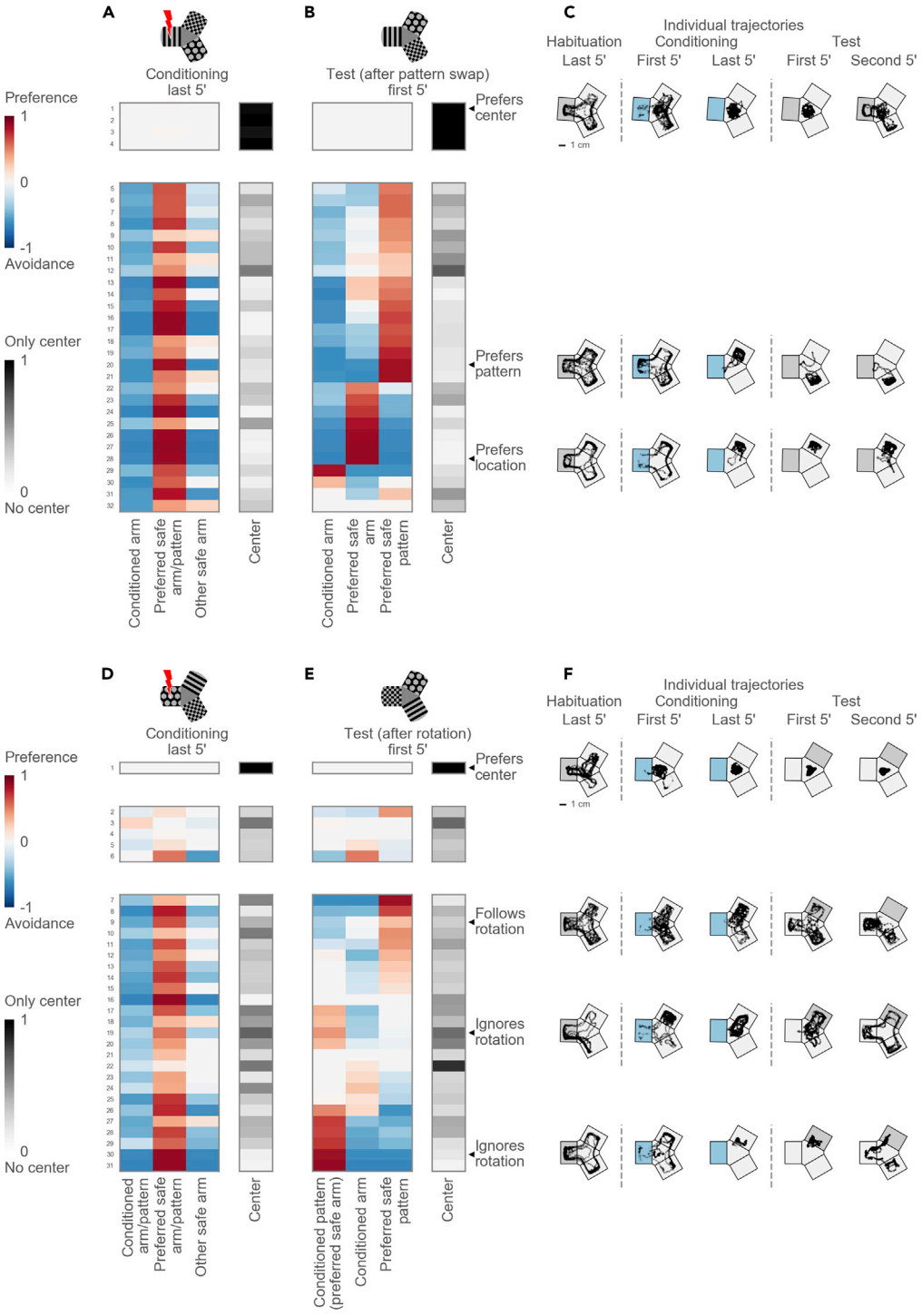

Figure 6. Dissociation of Pattern and Location Preference

(A) Top: schematic of the maze during the conditioning session in experiments with pattern swap. Bottom: hierarchical clustering reveals two groups: 4 center-preferring and 28 arm-avoiding fish.

(B) Arm occupancies during the test session in experiments with pattern swap. Occupancy groups correspond to the groups identified in (A).

(C) Example trajectories of individual fish before and after the pattern swap. Top: a fish prefers the center. Middle: a fish prefers one arm and switches the arm after the patterns are swapped. Bottom: another fish also prefers one arm but stays in the same arm after the pattern swap.

Figure 6. *Continued*

(D) Top: schematic of the maze during the conditioning session in experiments with pattern rotation. Bottom: hierarchical clustering reveals three groups: 1 center-preferring, 5 non-avoiding, and 25 avoiding fish.

(E) Arm occupancies during the test session in experiments with pattern rotation. The conditioned pattern moves into the preferred safe arm, thus creating a conflict between avoidance and preference cues. The pattern from the preferred arm moves into the non-preferred arm; the pattern from the non-preferred arm moves into the previously conditioned arm. Occupancy groups correspond to the groups identified in (D).

(F) Example trajectories of individual fish before and after the pattern rotation. Top: a fish prefers the center. Upper middle: a fish moves its preference following the preferred pattern and starts avoiding its previously preferred arm. Lower middle: a fish ignores the rotation and stays in its preferred arm despite the presence of the conditioned pattern. Bottom: another fish also ignores the rotation and stays in its preferred arm.

See also Figure S4.

HA swim bouts are less frequent than LA responses. Previous studies have shown that mild electric pulses directly activate Mauthner cells, bypassing sensory organs (Tabor et al., 2014). Such activation causes the fish to perform a C-bend, resembling the early stage of escape responses, a highly stereotyped tail movement (Liu et al., 2012; Temizer et al., 2015). The C-bend resembles the LA response types observed in this study. On the other hand, HA responses involve a series of powerful swim bouts and are more variable than LA responses. In contrast to LA responses, HA responses are followed on average by a more aversive response to conditioning; i.e., they are more effective as teaching signals (see Figure 4). One could speculate that the LA responses are triggered by direct activation of the Mauthner cell, as previously described, whereas HA responses are a result of activation of additional circuits in the brain. These could include sensory organs (e.g., lateral line, nociceptors) or additional reticulospinal neurons. Together, they might activate brain centers that encode the aversive quality of memories, such as dorsomedial telencephalon, a homologue of the mammalian basolateral amygdala (Mueller et al., 2011; Poulos et al., 2009). This observation suggests that electric shocks should be used as aversive stimuli with caution, as some types of observed reactions to shocks (LA) might be artifacts of direct activation of the Mauthner cell and might not have any perceptual or emotional saliency to the animal.

Experiments with identical visual patterns revealed that, on average, the absence of distinct visual patterns prevents the formation of conditioned responses (see Figure 3). This suggests that distinct visual patterns are necessary for learning in the CPA paradigm for the majority of the fish. This, however, does not exclude the possibility that a minority of fish (which only slightly influences the sample average) could use cues other than the projected patterns to avoid the conditioned arm.

Fish respond to conditioning with different navigational strategies. A subgroup of fish stays in the central compartment of the maze, avoiding all of the arms. This strategy is effectively the "safest haven," and does not require differentiation between the patterns. In this strategy, the fish could use the contrast between patterns in the arms and gray color of the central compartment as a cue for spatial learning; alternatively, the fish could use pattern-independent geometric perception of the central area as a part of the maze most removed from the walls (i.e., the center of the maze is a more open space). Another subgroup consists of fish preferring one or two safe arms, with the former being more common. A third subgroup consists of fish that failed to avoid the conditioned arm. This behavior is explained either by an insensitivity of the fish to electric shocks or by a failure to learn. We hypothesize that these diverse swimming patterns could be a result of associating different external cues with either punishment or safety (Figure 7). One-arm visitors could learn to seek one safe arm, using either its location cue or its visual pattern, whereas two-arm visitors could learn either to avoid the conditioned arm or to seek two safe arms.

When the conditioned pattern was replaced in the test session, most fish nevertheless continued to avoid the conditioned arm (see Figures 5D–5F). Thus, the strategy of using pattern avoidance as a learning cue is not sufficient to explain the avoidance behavior; rather, pattern avoidance is likely combined with a strategy of safety seeking, or avoiding transitions from a safe pattern to a punished location. The swap of two safe patterns after conditioning revealed that two-thirds of the fish prefer a safe pattern and switch their arm preference after the pattern swap, suggesting a strategy of learning a safe pattern. On the other hand, the other third prefer a safe location in the maze and stay in the same arm despite the pattern swap. The existence of location preference was further confirmed in experiments where all three patterns were rotated. There, some fish "rotate" their occupancy preferences together with the visual patterns, whereas other fish ignore the rotation, even when the

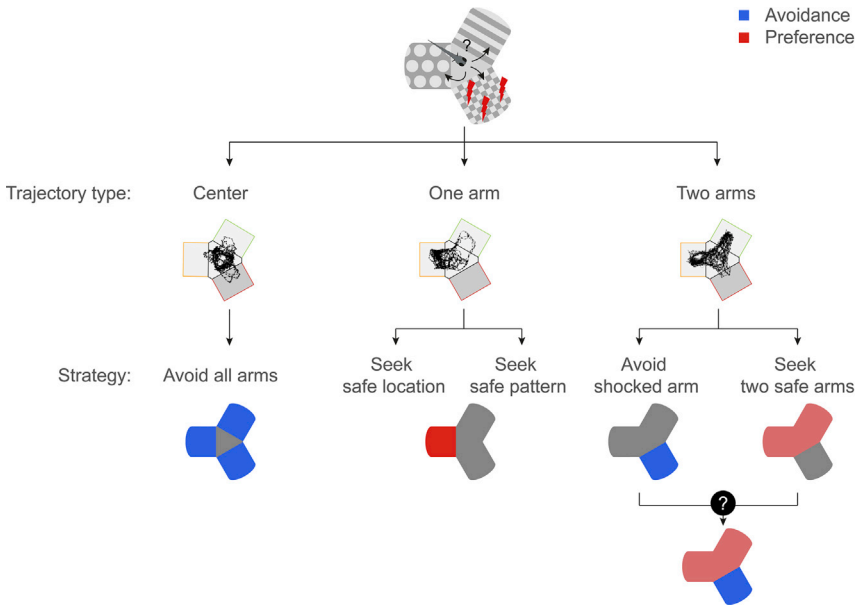

Figure 7. Diverse Strategies for Conditioned Place Avoidance Among Individual Animals

Center visitors could avoid all arms. One-arm visitors prefer one arm: either a pattern or a location in the maze. Two-arm visitors avoid the conditioned arm: either by avoiding the conditioned arm or by a more sophisticated strategy, e.g., learning the two safe patterns or the combination of visual and location cues in the maze.

conditioned pattern was rotated into the preferred arm of the fish (see Figure 6). Location-preferring fish could combine geometric cues in the maze, such as the corners of an arm, with an egocentric navigation strategy to stay within an arm. Such strategies are, however, prone to error accumulation: without any reference to stable external landmarks, animals tend to lose spatial orientation with time. In the case of radially symmetric Y-maze, animals that rely on an egocentric strategy but leave the preferred arm from time to time would rather quickly lose its location; this prediction agrees with the short-term memory of fish observed in our paradigm.

Such repertoire of strategies suggests individual flexibility in the spatial representation of safety. Previous studies suggested that each representation could be encoded by a different brain area (Broglio et al., 2010; O'Keefe and Dostrovsky, 1971; Packard and McGaugh, 1996; Salas et al., 2006). An exciting hypothesis is that these different representations together comprise a cognitive map of the environment, which stores the relationships between various cues and features (Tolman, 1948). Then, different parts of that map can be associated with safety or danger. When two cues come into conflict (e.g., when patterns are swapped or rotated and previously learned visual cues are dissociated from the geometry of the maze), a fish chooses one of the conflicting cues to execute the relevant behavior.

In conclusion, we have developed and explored a novel behavioral paradigm for studying spatial learning in juvenile zebrafish. Analysis of the population revealed robust and rapid learning, which depends on the presence of distinct visual cues. We uncovered several avoidance strategies, which indicate the presence of flexible neural mechanisms underlying the behavior. Recently developed techniques for embedding of juvenile zebrafish (Bergmann et al., 2018; Matsuda et al., 2017; Vendrell-Llopis and Yaksi, 2016), combined with immersive virtual reality setups, make juvenile zebrafish a promising model organism for future studies of brain activity in a navigating animal.

Limitations of the Study

In the described paradigm conditioning was performed within a single session, and aversive memory was investigated on a short-term timescale. Experiments with repeated conditioning sessions could create

stronger memory. Test for memory extinction on a longer timescale, as well as memory re-instatement test, could reveal additional dynamics in the learning/forgetting process. Although the presence of different navigation strategies is evident in zebrafish, the mechanisms behind these strategies will need further investigation. In particular, it is currently not clear to what extent the differences in strategies are innate as opposed to influenced by individual's experience.

METHODS

All methods can be found in the accompanying Transparent Methods supplemental file.

DATA AND CODE AVAILABILITY

Raw data, including coordinates of the fish in the maze, conditioning protocols, and Y-maze configurations are deposited in the Gin repository at https://web.gin.g-node.org/KseniaYashina/Zebramaze.

Analysis code is available in Bitbucket repository at https://bitbucket.org/mpinbaierlab/zebramaze/src/master/.

SUPPLEMENTAL INFORMATION

Supplemental Information can be found online at https://doi.org/10.1016/j.isci.2019.07.013.

ACKNOWLEDGMENTS

This work was funded by the Federal Ministry of Education and Research through the Bernstein Center for Computational Neuroscience Munich (01GQ1004A), the Max Planck Society, and the German Research Association (DFG) via the RTG 2175 "Perception in Context and its Neural Basis."

AUTHOR CONTRIBUTIONS

Conceptualization, K.Y., A.H., and H.B.; Methodology, K.Y., A.T.-C., A.H., and H.B.; Software, K.Y. and A.T.-C.; Validation, K.Y.; Formal Analysis, K.Y. and A.T.-C.; Investigation, K.Y.; Resources, H.B.; Data Curation, K.Y. and A.T.-C.; Writing – Original Draft, K.Y., A.H., and H.B.; Writing – Review & Editing, K.Y., A.T.-C., A.H., and H.B.; Visualization, K.Y.; Supervision, A.H. and H.B.; Project Administration, K.Y., A.H., and H.B.; Funding acquisition, A.H. and H.B.

DECLARATION OF INTERESTS

The authors declare no competing interests.

Received: May 14, 2019
Revised: July 3, 2019
Accepted: July 10, 2019
Published: September 27, 2019

REFERENCES

Aizenberg, M., and Schuman, E.M. (2011). Cerebellar-dependent learning in larval Zebrafish. J. Neurosci. *31*, 8708–8712.

Al-Imari, L., and Gerlai, R. (2008). Sight of conspecifics as reward in associative learning in zebrafish (*Danio rerio*). Behav. Brain Res. *189*, 216–219.

Aoki, R., Tsuboi, T., and Okamoto, H. (2015). Y-maze avoidance: an automated and rapid associative learning paradigm in zebrafish. Neurosci. Res. *91*, 69–72.

Bergmann, K., Meza Santoscoy, P., Lygdas, K., Nikolaeva, Y., MacDonald, R., Cunliffe, V., and Nikolaev, A. (2018). Imaging neuronal activity in the optic tectum of late stage larval Zebrafish. J. Dev. Biol. *6*, 6.

Braubach, O.R., Wood, H.-D., Gadbois, S., Fine, A., and Croll, R.P. (2009). Olfactory conditioning in the zebrafish (*Danio rerio*). Behav. Brain Res. *198*, 190–198.

Broglio, C., Rodríguez, F., Gómez, A., Arias, J.L., and Salas, C. (2010). Selective involvement of the goldfish lateral pallium in spatial memory. Behav. Brain Res. *210*, 191–201.

Cheng, K. (1986). A purely geometric module in the rat's spatial representation. Cognition *23*, 149–178.

Durán, E., Ocaña, F.M., Broglio, C., Rodríguez, F., and Salas, C. (2010). Lateral but not medial telencephalic pallium ablation impairs the use of goldfish spatial allocentric strategies in a "hole-board" task. Behav. Brain Res. *214*, 480–487.

Eichenbaum, H. (2017). The role of the hippocampus in navigation is memory. J. Neurophysiol. *117*, 1785–1796.

Fanselow, M.S. (1990). Factors governing one-trial contextual conditioning. Anim. Learn. Behav. *18*, 264–270.

Franz, M.O., and Mallot, H.A. (2000). Biomimetic robot navigation. Rob. Auton. Syst. *30*, 133–153.

Gouteux, S., Thinus-Blanc, C., and Vauclair, J. (2001). Rhesus monkeys use geometric and nongeometric information during a reorientation task. J. Exp. Psychol. Gen. *130*, 505–519.

Harmon, T.C., Magaram, U., McLean, D.L., and Raman, I.M. (2017). Distinct responses of Purkinje neurons and roles of simple spikes during associative motor learning in larval zebrafish. Elife *6*. https://doi.org/10.7554/eLife.22537.

Hinz, F.I., Aizenberg, M., Tushev, G., and Schuman, E.M. (2013). Protein synthesis-dependent associative long-term memory in larval Zebrafish. J. Neurosci. *33*, 15382–15387.

Kalueff, A.V., Gebhardt, M., Stewart, A.M., Cachat, J.M., Brimmer, M., Chawla, J.S., Craddock, C., Kyzar, E.J., Roth, A., Landsman, S., et al. (2013). Towards a comprehensive catalog of Zebrafish behavior 1.0 and beyond. Zebrafish *10*, 70–86.

Kelly, D.M., Spetch, M.L., and Heth, C.D. (1998). Pigeons' (*Columba livia*) encoding of geometric and featural properties of a spatial environment. J. Comp. Psychol. *112*, 259–269.

Kenney, J.W., Scott, I.C., Josselyn, S.A., and Frankland, P.W. (2017). Contextual fear conditioning in zebrafish. Learn. Mem. *24*, 516–523.

Lal, P., Tanabe, H., Suster, M.L., Ailani, D., Kotani, Y., Muto, A., Itoh, M., Iwasaki, M., Wada, H., Yaksi, E., and Kawakami, K. (2018). Identification of a neuronal population in the telencephalon essential for fear conditioning in zebrafish. BMC Biol. *16*, 45.

Lee, A., Mathuru, A.S., Teh, C., Kibat, C., Korzh, V., Penney, T.B., and Jesuthasan, S. (2010). The Habenula prevents helpless behavior in larval Zebrafish. Curr. Biol. *20*, 2211–2216.

Lee, S., Vallortigara, G., Ruga, V., and Sovrano, V. (2012). Independent effects of geometry and landmark in a spontaneous reorientation task: a study of two species of fish. Anim. Cogn. *15*, 861–870.

Lee, S., Vallotigara, G., Flore, M., Spelke, E., and Sovrano, V. (2013). Navigation by environmental geometry: the use of zebrafish as a model. J. Exp. Biol. *216*, 3693–3699.

Lee, S., Ferrari, A., Vallortigara, G., and Sovrano, V. (2015). Boundary primacy in spatial mapping: evidence from zebrafish (Danio rerio). Behav. Processes *119*, 116–122.

Liu, Y.-C., Bailey, I., and Hale, M.E. (2012). Alternative startle motor patterns and behaviors in the larval zebrafish (*Danio rerio*). J. Comp. Physiol. A *198*, 11–24.

López, J.C., Bingman, V.P., Rodríguez, F., Gómez, Y., and Salas, C. (2000). Dissociation of place and cue learning by telencephalic ablation in goldfish. Behav. Neurosci. *114*, 687–699.

López, J.C., Broglio, C., Rodríguez, F., Thinus-Blanc, C., and Salas, C. (1999). Multiple spatial learning strategies in goldfish (*Carassius auratus*). Anim. Cogn. *2*, 109–120.

Matsuda, K., Yoshida, M., Kawakami, K., Hibi, M., and Shimizu, T. (2017). Granule cells control recovery from classical conditioned fear responses in the zebrafish cerebellum. Sci. Rep. *7*, 11865.

Mueller, T., Dong, Z., Berberoglu, M.A., and Guo, S. (2011). The dorsal pallium in zebrafish, *Danio rerio* (Cyprinidae, Teleostei). Brain Res. *1381*, 95–105.

O'Keefe, J., and Dostrovsky, J. (1971). The hippocampus as a spatial map. Preliminary evidence from unit activity in the freely-moving rat. Brain Res. *34*, 171–175.

Packard, M.G., and McGaugh, J.L. (1996). Inactivation of Hippocampus or caudate nucleus with lidocaine differentially affects expression of place and response learning. Neurobiol. Learn. Mem. *65*, 65–72.

Poulos, A.M., Li, V., Sterlace, S.S., Tokushige, F., Ponnusamy, R., and Fanselow, M.S. (2009). Persistence of fear memory across time requires the basolateral amygdala complex. Proc. Natl. Acad. Sci. U S A *106*, 11737–11741.

Salas, C., Broglio, C., Durán, E., Gómez, A., Ocaña, F.M., Jiménez-Moya, F., and Rodríguez, F. (2006). Neuropsychology of learning and memory in teleost fish. Zebrafish *3*, 157–171.

Sison, M., and Gerlai, R. (2010). Associative learning in zebrafish (*Danio rerio*) in the plus maze. Behav. Brain Res. *207*, 99–104.

Tabor, K.M., Bergeron, S.A., Horstick, E.J., Jordan, D.C., Aho, V., Porkka-Heiskanen, T., Haspel, G., and Burgess, H.A. (2014). Direct activation of the Mauthner cell by electric field pulses drives ultrarapid escape responses. J. Neurophysiol. *112*, 834–844.

Temizer, I., Donovan, J.C., Baier, H., and Semmelhack, J.L. (2015). A visual pathway for looming-evoked escape in larval Zebrafish. Curr. Biol. *25*, 1823–1834.

Tolman, E.C. (1948). Cognitive maps in rats and men. Psychol. Rev. *55*, 189–208.

Valente, A., Huang, K.-H., Portugues, R., and Engert, F. (2012). Ontogeny of classical and operant learning behaviors in zebrafish. Learn. Mem. *19*, 170–177.

Vallortigara, G., Zanforlin, M., and Pasti, G. (1990). Geometric modules in animals' spatial representations: a test with chicks (*Gallus gallus* domesticus). J. Comp. Psychol. *104*, 248–254.

Vargas, J.P., López, J.C., Salas, C., and Thinus-Blanc, C. (2004). Encoding of geometric and featural spatial information by Goldfish (*Carassius auratus*). J. Comp. Psychol. *118*, 206–216.

Vendrell-Llopis, N., and Yaksi, E. (2016). Evolutionary conserved brainstem circuits encode category, concentration and mixtures of taste. Sci. Rep. *5*, 17825.

Yang, W., Meng, Y., Li, D., and Wen, Q. (2019). Visual contrast modulates operant learning responses in larval Zebrafish. Front. Behav. Neurosci. *13*, 4.

ISCI, Volume *19*

Supplemental Information

Zebrafish Exploit Visual Cues and Geometric Relationships to Form a Spatial Memory

Ksenia Yashina, Álvaro Tejero-Cantero, Andreas Herz, and Herwig Baier

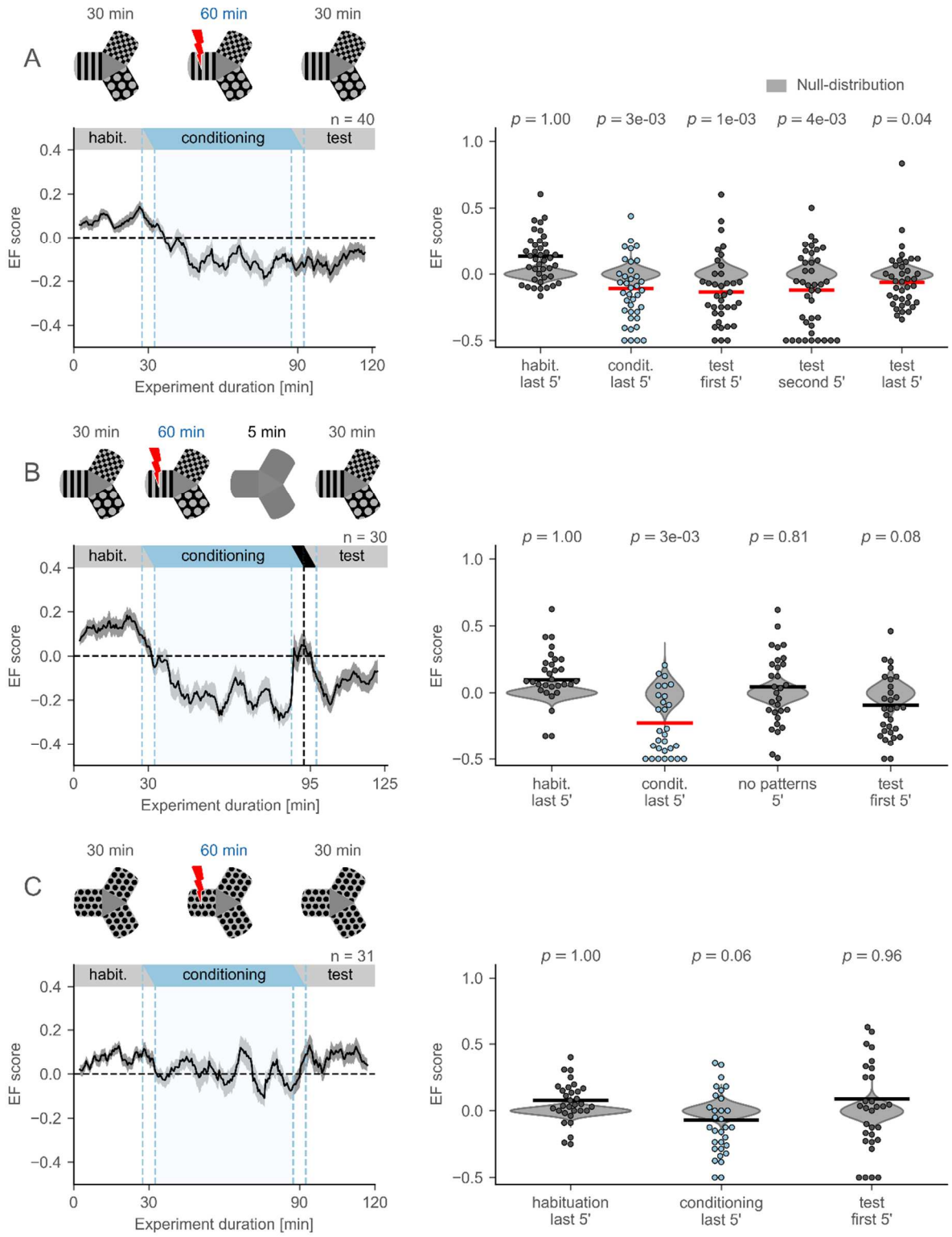

Figure S1. Analysis of the entry frequency score. Related to Figure 3.

(A) Top: schematic of the protocol with habituation, conditioning, and test sessions. Bottom, left: EF score moving average. Right: comparison of EF scores in the last 5 min of conditioning and the first, second, and last 5 min of test session with the null-distribution (permutation test, n = 40 fish). **(B)** Top: schematic

of the protocol with habituation, conditioning, no-pattern, and test sessions. Bottom, left: EF score moving average. Bottom, right: comparison of EF scores in the last 5 min of conditioning, 5 min of no-pattern, and in the first 5 min of test session with the null-distribution (permutation test, n = 30 fish). **(C)** Top: schematic of the protocol where visual patterns in all arms are identical. Bottom, left: EF score moving average. Bottom, right: comparison of EF scores in the last 5 min of conditioning and the first 5 min of test session with the null-distribution (permutation test, n = 31 fish). All annotations are the same as in Figure 3.

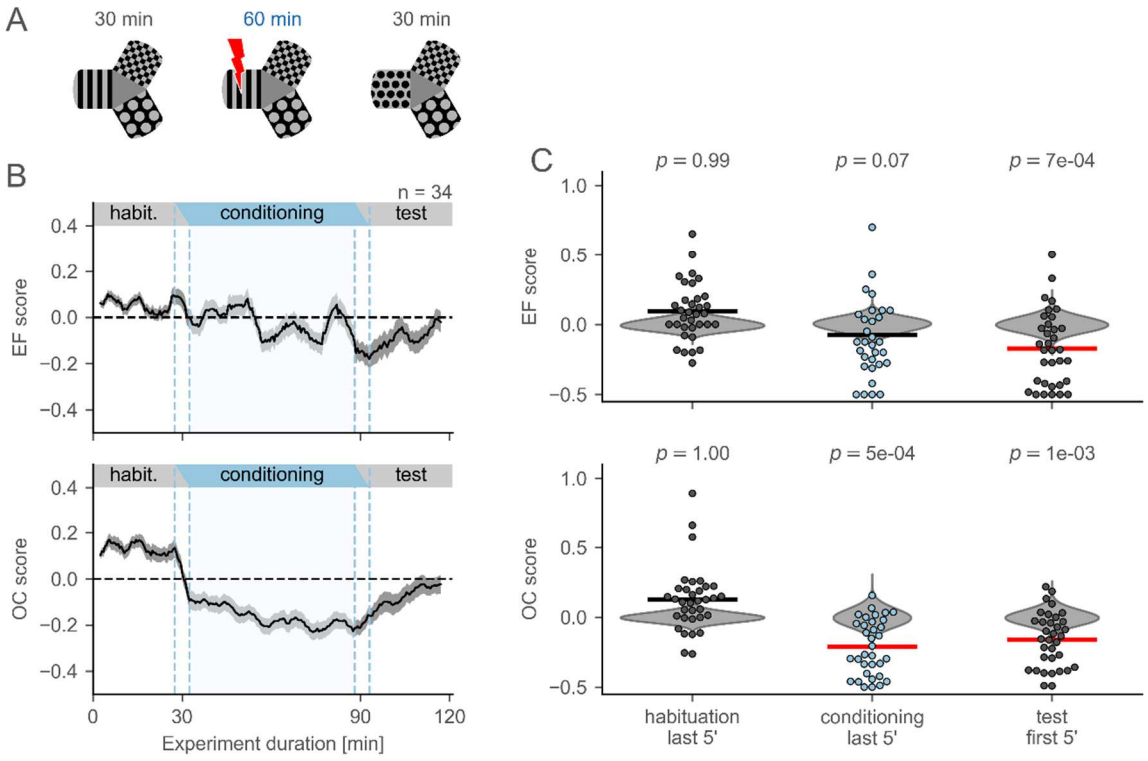

Figure S2. Zebrafish continue to avoid conditioned arm after replacement of conditioned pattern. Related to Figure 5.

(A) Schematic of the protocol with the replacement of the conditioned pattern in the test session. **(B)** EF (top) and OC (bottom) score moving averages. **(C)** Comparison of the EF (top) and OC (bottom) scores in the last 5 min of conditioning and in the first 5 min of test session with the null-distribution (permutation test, n = 34 fish).

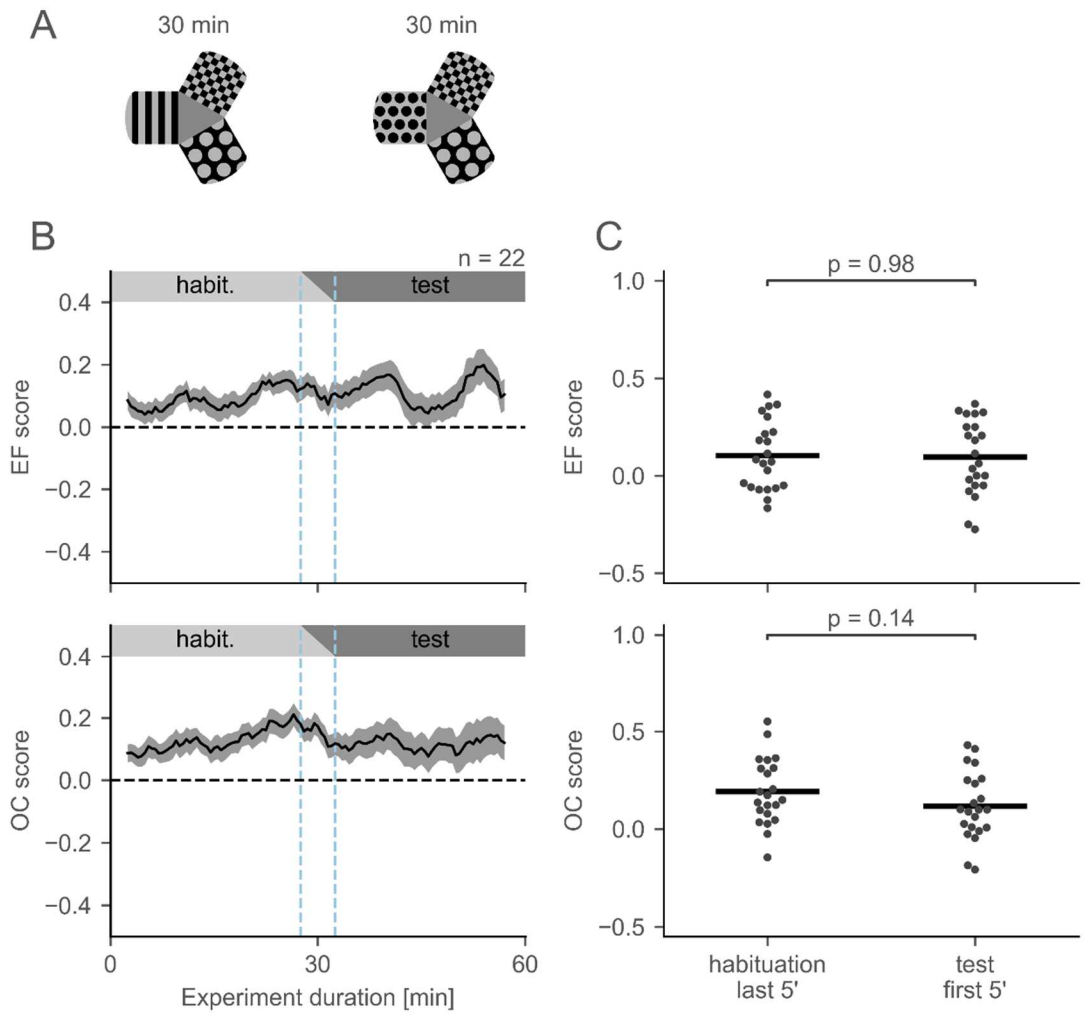

Figure S3. Pattern replacement is neither intrinsically aversive nor attractive to fish. Related to Figure 5.

(A) Schematic of the control protocol with habituation and test sessions. The pattern in the preferred arm was replaced in the test session. **(B)** EF (top) and OC (bottom) score moving averages. **(C)** Comparison of the EF (top) and OC (bottom) scores between the last 5 min of conditioning and the first 5 min of the test session (two-sided Mann-Whitney test, n = 22 fish). Dots show OC/EF score values of individual fish.

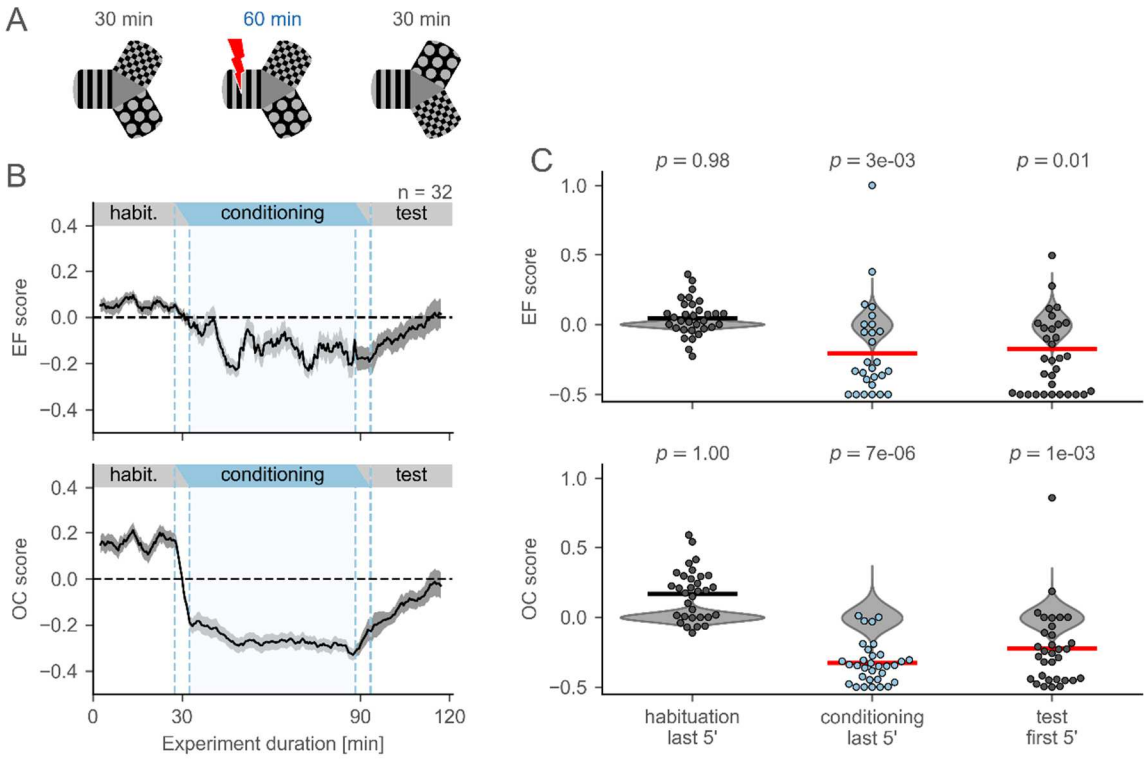

Figure S4. Zebrafish continue to avoid conditioned arm after swap of safe patterns. Related to Figure 6.

(A) Schematic of the protocol with the swap of the safe patterns in the test session. **(B)** EF (top) and OC (bottom) score moving averages. **(C)** Comparison of the EF (top) and OC (bottom) scores in the last 5 min of conditioning and in the first 5 min of the test session with the null-distribution (permutation test, n = 32 fish).

Table S1. Animals used in all experimental protocols. Related to Figure 1.

Experiment	Used in analysis	Excluded: overstayers	Excluded: unstable	Excluded: froze	Total	Age [dpf*]
Age comparison: 1 week	13	4	1	0	18	8
Age comparison: 2 weeks	10	7	0	0	17	14-16
Age comparison: 3 weeks	16	7	0	0	23	21-23
Control	24	--	--	--	24	22
Three patterns + test	40	13	6	4	63	21-25
Three patterns + no-patterns + test	30	9	1	0	40	20-24
Identical patterns	31	18	2	3	54	22-23
Swap of safe patterns	32	16	0	5	53	20-27
Replacement of shocked pattern	34	21	2	10	67	20-25
Control: pattern replacement	22	--	--	--	22	21-23
Rotation	31	14	3	8	56	21-23
Total	283	109	15	30	437	

Dpf – days post fertilization

Transparent Methods

Experimental model and subject details

Wild-type zebrafish of strain Tupfel Longfin (TL) were maintained at 28 degrees on a 14h-10h light-dark cycle. Embryos were obtained by spawning three adult fish pairs simultaneously. Embryos were raised in Danieau's buffer (17 mM NaCl, 2 mM KCl, 0.12 mM $MgSO_2$, 1.8 mM $Ca(NO_3)_2$, 1.5 mM HEPES) for the first 5 days of development. At 6 days post fertilization (dpf) the larvae were transferred to 3.5l tanks with fish system water (approx. 30 animals per tank). From 6 dpf to 20 dpf they were fed twice a day with live Rotifers and dry algae powder (Tetra Aufzuchtsfutter). From day 20 onwards, the diet was smoothly changed to a combination of freshly hatched artemia and Gemma micro dry food (Skretting). Animals were taken out of the fish facility and into the behavior room directly before the start of each experiment. Animals between the age of 8 and 27 dpf were used in the experiments. Males and females were not discriminated as the gonadal differentiation happens at a later stage of development. All animal procedures were conducted in accordance with the institutional guidelines of the Max Planck Society and the local government (Regierung von Oberbayern, animal license 55.2-1-54-2532-108-2016).

Experimental setup

The setup was custom-built in the lab. The walls and bottom of the Y-maze were laser-cut out of cast acrylic. The maze arms had a 1:1 width-to-length ratio, with a length of 30 mm; the walls were 10 mm high. Each arm opened to the triangular center of the maze, the ends of the arms were rounded. We used two identical mazes in parallel to allow the testing of two fish simultaneously, and therefore increasing the throughput. Walls of the two mazes were opaque to prevent fish from seeing each other during the experiment. Each maze had a piece of diffusive paper underneath for back projection of the visual stimuli (Rosco, Tough Rolux 3000). Both mazes and the diffusive paper were placed into a water basin, in order to remove the additional air layer between the screen and the fish and reduce light refraction. The scene was illuminated from below with a custom-built infra-red (IR) LED array to allow behavioral imaging. Both mazes were positioned under a high-speed camera (Ximea USB3.0 model MQ013MG-ON), in such a way that the walls did not produce a vertical shadow. The camera had a 6 mm lens (Thorlabs, Cat #MVL16M23) and an IR filter to filter out transmitted visible light. The setup was surrounded with black, opaque walls to shield the fish from distracting visual cues in the room.

Visual stimuli, designed in Python, were projected onto the diffusive paper with an LED-projector (LG model PA70G) via a cold mirror (Edmund Optics Cat # 64-452). The mirror was positioned at 45^o allowing IR light from below to pass through and light from the projector to be reflected onto the diffusive screen, as shown in Figure 1A. Stimuli were projected under the arms of the maze. The projected stimuli included (a) a pattern with black dots on light gray background; (b) a pattern with light gray dots on black background; (c) a pattern with black and light gray stripes; (d) a checkered pattern of black and light gray colors; (e) uniform gray (RGB = (128, 128, 128)). The light gray color was used instead of white to lower the brightness of the arena as high brightness could increase stress levels of the fish (personal observations). The patterns were designed such that the light-to-dark ratio was 1:1 in order to prevent differences in luminance between the stimuli, as larval zebrafish exhibit phototactic behavior (Burgess and Granato, 2007; Orger et al., 2000). The central area always had a uniform gray color (RGB = (135, 135, 135)), which was different from the gray in the arms to ensure that there was a contrast border at the entrance to the arms. Light gray RGB value was (180, 180, 180), black RGB value was (0, 0, 0).

Each arm contained a pair of electrodes located at the side walls. Each electrode was shaped as a 30-by-10 mm rectangle made out of steel mesh with wire diameter 0.2 mm, aperture 0.5 mm (Mijo Ilic Drahtgewebe-Shop.de) and covered the entire side wall. The electrodes were connected to a constant current stimulator (Digitimer DS3). Electrical stimulation was applied at 1 Hz in the periods between the entry and the exit of the fish from the conditioned arm. Electric pulses lasted between 50 and 100 ms, depending on the experiment (we did not observe differences in responses to shocks with these pulse lengths). Pulse amplitude was 0.7 mA (the value was chosen to elicit visible responses to the electric stimulus in all animals). The water used in the experiments was obtained from the fish facility (pH 7.5, temperature 28^{o}C, conductivity 650 µS).

Experimental protocols

Each experimental protocol consisted of one or more experimental sessions. The sessions followed each other without interruption, and each session could be characterized by its duration, the visual patterns that were projected onto the bottom of the Y-maze, and the ON/OFF status of the electric stimulation. In each protocol, every fish was tested individually and only once. 437 fish were tested in total.

Experiment was interrupted if a fish spent longer than one minute in the conditioned arm of the maze (equivalent to experiencing 60 shock pulses). This was done to prevent excessive stress for the animals. 109 fish were excluded from the analysis based on this criterion.

15 fish that did not reach a stable OC score (see "Measures for the CPA paradigm" below) at the end of conditioning were excluded from the analysis. The score was considered stable if the last point of the moving average lied within the 95th percentile range of the last 10 points of the moving average.

Finally, 30 fish that showed freezing behavior as a result of conditioning were also excluded from the analysis. Freezing behavior was identified by the 5th percentile of the distribution of total distance moved across all fish.

Overall, the analyzed dataset included 283 fish (see Table S1 for detailed numbers).

Behavioral tracking

All tracking was performed using custom-written code in Python, including the OpenCV library (Bradski, 2000). Black-and-white images were recorded at 60 fps with a resolution of 0.14mm per pixel. The position of the fish was identified in real-time using background subtraction. The background was calculated as a running average of the last 20 seconds of the recording. This time-dependent background was subtracted from the current frame, the result was filtered with a Gaussian filter with a 5x5 pixel kernel to remove point pixel noise, and then binary thresholded. The fish was identified as the contour with the largest area on the thresholded image. Fish position was calculated as the center of mass of the corresponding contour. The identified position was corrected using a Kalman filter to reduce the noise in the recordings (Kalman, 1960). Filter state variable included (x, y) position of the fish and x- and y-projections of the speed, and was updated for every frame of the recording using the observed fish position. Filter model for motion assumed movement with constant speed. Noise along x- and y-coordinates was assumed to be independent.

Swim bouts in Figure 1E were estimated from the time series of fish positions in the maze after the experiment by analyzing the recorded videos. First, speed of the fish was calculated as the Euclidean distance between positions at adjacent time frames. The speed was then filtered using a finite impulse response filter with a low-pass kernel (Parks–McClellan algorithm with 4Hz cutoff frequency) to remove high-frequency noise (Parks and McClellan, 1972). Swim bouts were defined as intervals of the filtered speed curve above a manually set threshold. The swim bout amplitude was calculated by integrating the area under the speed curve between the boundaries of the bout.

The fish's heading direction in Figure 4 was calculated for each frame of the recorded video. First, a contour of the fish was identified in a manner similar to the calculation during the experiment as described above. The terminal point of the heading vector was at the center of mass of the contour, which roughly corresponded to the head of the fish. The initial point of the vector was at the furthermost point of the contour from the center of mass, which corresponded to the tail tip of the fish. The heading direction was calculated as a relative angle between the heading vector and the horizontal edge of the image. Fish's orientation in the arm was calculated as a relative angle between the heading direction of the fish and the orientation of the arm. The orientation of the arm was given by the arm vector, whose initial point was at the maze center, and whose terminal point was at the arm center. Arm orientation was identified as an angle between the arm vector and the horizontal edge of the image. Fish's orientations in the arm were divided into four categories: "into the arm" for angles between -45^o and 45^o; "towards the anode" for angles between 45^o and 135^o; "out of the arm" for angles between 135^o and 225^o; "towards the cathode" for angles between 225^o and 315^o. "Towards the anode" and "towards the cathode" orientations were called aligned with the electric field, while "into the arm" and "out of the arm" orientations were called misaligned with the electric field.

Fish size was calculated as the Euclidean distance between the tip of the head and the tip of the tail, whose positions were manually picked by analyzing recorded videos. To reduce the assessment noise, the length was identified in five randomly picked frames of the video for each fish. Afterwards the final length was obtained by averaging the five handpicked lengths. The accuracy of this procedure was estimated with a coefficient of variation of fish size, calculated for every fish by dividing the standard deviation of manually measured fish lengths by the mean of those lengths. Coefficients of variation were calculated for a random sample of all experimentally tested fish (n = 42). The obtained values did not exceed 5%.

Measures for the CPA paradigm

Behavior in the CPA paradigm was assessed with two measures: occupancy of the arms (OC) and entry frequency of the arms (EF). OC of a particular arm, or maze center, was calculated as the proportion of time spent in the respective part of the maze. EF of a particular arm was calculated by dividing the number of times that the fish entered into that arm by the total amount of entries the fish performed into all arms. The two measures could be calculated for the whole time of an experiment as well as for a part of an experiment (in a corresponding time window).

We created a preference score in order to estimate learning effects. The score was calculated for each measure separately as the difference between the mean OC/EF of the conditioned arm and the average of OC/EF of the other two arms (Equation 1 for the occupancy score, OC_{score}, and Equation 2 for the entry frequency score, EF_{score}). Score values were above zero when the conditioned arm was preferred, and below zero when the arm was avoided. Note that the OC_{score} is calculated from the OC-values of the three arms, irrespective of the OC-value of the maze center.

$$OC_{score} = OC_{shock} - \frac{1}{2}\left(OC_{safe1} + OC_{safe2}\right) \quad (1)$$

$$EF_{score} = EF_{shock} - \frac{1}{2}\left(EF_{safe1} + EF_{safe2}\right) \quad (2)$$

The dynamics of the preference score throughout an experiment were visualized using moving average with a 5-minute time window and a 30-second step, i.e. two adjacent windows had a 4.5-minute overlap. Every point on the moving average represents the average OC/EF score across individual fish in a single time window. Error bars for the moving average correspond to the standard error of the mean. Some points of the moving average were calculated from the data of two adjacent sessions (sessions can have different experimental conditions, i.e. ON/OFF electric stimulation); vertical dashed lines mark intervals reflecting mixed experimental conditions.

As individual fish could have different number of arm entries within a 5-minute time window (e.g. because of different swimming speeds), we calculated the weighted average across individual fish for the EF score. The weights were proportional to the total number of entries for a particular fish in a particular time window.

Permutation test

Permutation test was used to assess the differences between the OC/EF measures in the conditioned arm and the other two arms of the maze. For each experimental protocol, a permutation test was performed for the last 5 minutes of the conditioning session (to estimate the effects of shocks during the conditioning) and for the first 5 minutes of the test session (to estimate the memory of the conditioning after the electric stimulation was switched off). OC/EF of each arm for each fish were calculated in these time windows. Then, for each fish separately, the arms were randomly relabeled, so that the OC/EF values were reassigned to different arms. Such relabeling (permutation) was performed $n = 10^6$ times. Preference score was then calculated for the experimental values and for each permutation as described above. OC/EF scores obtained from all permutations constitute a distribution of score values for the null hypothesis, i.e. that all arms are interchangeable for the fish, and therefore that there is no significant difference between the OC/EF of the conditioned arm and the other two arms. The experimental score value lies somewhere in this distribution. The significance of the experimental score value is assessed by calculating its position in the null-distribution (Equation 3).

$$p_{value} = P(Score^{null} \leq Score^{exp}) \qquad (3)$$

In the cases of very strong effects of conditioning sometimes none of the permutations produced a score lower than the experimental value. In such cases, the estimated *p*-value was equal to 0. In order to get an informative value, we fitted a Gaussian to the null-distribution, and calculated the probability of the experimental value to occur against the Gaussian. This Gaussian estimated *p*-value is reported for the experiments.

Clustering of shock-triggered swim bouts

The dataset for shock-triggered swim bouts in Figure 4 was obtained from the conditioning sessions of 27 fish. It contained responses to 14,519 shocks, each shock was 67 ms long. For every shock, fish coordinates were extracted for the 35-second interval starting at the shock onset. Every coordinate sequence was then transformed into frame-to-frame speed sequence, calculated from the Euclidean distances between coordinates from adjacent time frames. Every speed curve was smoothed using univariate splines. Speeds whose peak values were lower than a threshold value of 21.4 mm/s were considered non-responses (n = 10,428); the rest were considered swim bouts (n = 4,091). This threshold was chosen such that automatically and visually identified swim bouts matched (data not shown). Additionally, we calculated the orientation of the fish in the conditioned arm at the onset of each identified swim bout.

Principal-component analysis was performed on the dataset of smoothed bout speed curves in order to identify their important features (Jolliffe, 2002). Four principal components could explain more than 90% of total variance in the dataset, and were selected as the main features of the speed curves. Hierarchical clustering with Ward's linkage method was performed on a bout dataset, which was represented by a 4,091-by-4 matrix (4 principal components per bout, orientation in the arm was not included as a parameter for the clustering). Ward's linkage method minimizes the sum-of-squares within the clusters (Ward, 1963). The cut level for the cluster tree was chosen so that three clusters emerge. Every cluster was considered to represent a separate type of response to shocks.

Comparison of avoidance levels between different response types was performed using the one-way Kruskal-Wallis test, followed by a post-hoc Mann-Whitney test for group comparisons. Three response types were compared against each other (3 pairs). The avoidance levels were estimated by calculating the OC/EF scores in the next 5 minutes after every individual shock response of a particular type.

Separation of avoidance strategies

Avoidance strategies in Figure 5 and Figure 6 were estimated using hierarchical clustering with Ward's linkage of the arm occupancies in the last 5 minutes of conditioning. For each fish, we computed the occupancy of each arm as described above and re-centered them around zero (so that they sum up to zero). Negative arm occupancy means avoidance, and positive arm occupancy corresponds to preference of the arm. Additionally, we calculated the occupancy of the center. As a result, for each fish a vector of 4 values was calculated: 3 corrected arm occupancies and 1 center occupancy. Importantly, the three occupancies for the arms were linearly dependent, so we excluded one of the arms in clustering. In total, clustering was applied to a 179x3 occupancy matrix, where 179 rows corresponded to individual fish (note that we used fish pooled from different experiments with identical conditioning sessions). Before clustering, values within each column were standardized by centering around the mean and scaling to unit variance.

At each node of the clustering dendrogram, we estimated the significance of splitting the subtree under that node into two clusters. For any current subtree we permuted occupancy values within the columns of the corresponding occupancy matrix (10^4 permutations in total). We used the same clustering method to get two clusters for each permutation, and obtained linkage values between these two clusters. These linkage values formed a null-distribution corresponding to the hypothesis that there is no separation of the subtree at the investigated node. Then, the position of the original, non-permuted, linkage value was identified in the null-distribution. The significance threshold was chosen to accommodate multiple comparisons between different subtrees of one dendrogram. Briefly, for the node J the significance value

p^J_{value} was adjusted by dividing the chosen significance level (0.05) by the number of nodes between the current node and the root of the dendrogram, D_J (Equation 4).

$$p^J_{value} = p_{value} \cdot \frac{1}{D_J} \quad (4)$$

Statistical significance of cluster separation was estimated recursively, starting from the root and investigating each of the following two subtrees. Using this method, we identified six statistically significant clusters. For visualization and explanation purposes, we combined four clusters with the lowest occupancy of the conditioned arm into the 'arm-avoiding' group, while the other two clusters corresponded to 'non-avoiding' and 'center-preferring' groups (see Figures 5 and 6).

Memory-less model

A pseudo-random walk model in Figure 1 was designed to investigate how reactions to shocks, independent of learning, could influence the OC and EF measures of the conditioned arm. In the model, the arms of the Y-maze were reduced to three one-dimensional (1D) linear tracks. Each 1D arm had a length (parameter *L*) and a coordinate axis associated with it, with the arm opening located at 0, and the arm end located at a distance *L* from the origin. The center of the maze was modeled as a separate 1D compartment of length L_{center}. The simulated agent moved along the arm axis with discrete steps (bouts). Each step had a direction (towards the left or the right boundary of the arm) and a size *S*. In order to choose the step size *S*, we used the experimentally observed distribution of swim bout amplitudes (Figure 1E, gray). The experimental distribution was fitted with a Gamma distribution (equation 5) with shape parameter $k = 1.958$ and scale parameter $\theta = 0.999$ mm.

$$f(x,k,\theta) = \frac{x^{k-1}\exp(-\frac{x}{\theta})}{\theta^k \Gamma(k)}, \qquad \text{where} \quad \Gamma(z) = \int_0^\infty x^{z-1}e^{-x}dx \quad (5)$$

The mean of the fitted distribution, calculated as a product of shape and scale parameters, was equal to 1.956 mm. Thus the average swim bout amplitude, relative to the maze arm length (30 mm), was 1.956 mm/30 mm = 0.065. In order to match these parameters in the model, we drew the step size *S* from a Gamma distribution with mean of $0.065 \cdot L$, where *L* was the length of the arm in the modeled maze. Similarly, in terms of *L*, the scale parameter θ can be written as $\theta = 0.999 \text{ mm} \cdot L/30 \text{ mm} = 0.033 \cdot L$.

If the simulated agent moved beyond the left arm boundary, it exited its current arm and entered the central compartment. When the simulated agent moved to the right arm boundary, it stopped there until the next step of the simulation ('sticky' boundary conditions). Both boundaries of the central compartment were treated equally: if the simulated agent stepped over either the left or the right boundary of the central compartment, it entered an arm. Each arm had a probability of entry associated with it, all probabilities summing to one. The effects of the electric shocks could be simulated in one of the arms. The size of every step made in the shocked arm was multiplied by a parameter $\alpha \geq 1$, to simulate the increased swimming speed in response to electric shocks.

The model without learning was used to investigate if the increased speed in the conditioned arm alone could explain the changes in OC/EF measures during conditioning. An experiment was simulated with 3 sessions. Each session lasted *n* steps. In the starting habituation session, the step sizes *S* of the simulated agent in all arms were drawn from the same Gamma distribution. At the end of the habituation session, the arm with the highest occupancy was selected as the conditioned arm for the following conditioning session (occupancy was higher in one arm due to stochastic reasons). In the conditioning session, the sampled step size *S* of the simulated agent in the conditioned arm was multiplied by the parameter $\alpha > 1$ to simulate increased speed during the shocks. In the third (test) session, step sizes in all of the arms were again drawn from the same distribution. Probabilities of entry into any of the arms were equal to 1/3 in all sessions. All simulations were run using custom Python code. Parameters used for simulations in Fig 1: $L = 5$; $L_{\text{center}} = 1.5$; $k = 1.96$, $\theta = 0.033 \cdot 5 = 0.165$; $\alpha = \{1, 2, 3, 4\}$; $n_{\text{habituation}} = 20{,}000$ steps; $n_{\text{conditioning}} = 40{,}000$ steps; $n_{\text{test}} = 20{,}000$ steps.

A learning component was added to the model to investigate if the learning measures can be used to detect learning effects. In the model with learning, the probability of entry into the arms of the simulated

maze was changed from a constant to a variable parameter. Under the learning rule, each entry into the conditioned arm during conditioning decreased the probability of returning to that arm. This rule corresponded to an exponential decay of the probability of entry, with a learning rate β and a floor of 0.1 (a non-zero value was chosen because in the experiments the probability of entry never reduced to 0, Equation 6). The probabilities of entry into the other two arms increased correspondingly, to keep the sum of all probabilities equal to one (Equations 7 and 8).

$$\Delta p_{entry}^{shock} = \beta \cdot \left(0.1 - p_{entry}^{shock}\right) \quad (6)$$

$$\Delta p_{entry}^{non-shock} = -\frac{1}{2} \cdot \Delta p_{entry}^{shock} \quad (7)$$

$$\sum_{all\ arms} p_{entry} = 1 \quad (8)$$

Memory extinction in the test session was simulated by slowly letting the probability of entry into the conditioned arm rise back to the 1/3 level (Equation 9). The update of the probability occurred at every return to the previously conditioned arm. The probabilities of entry into the other two arms were decreased correspondingly (Equation 10 and 11)

$$\Delta p_{entry}^{shock} = \beta \cdot \left(0.33 - p_{entry}^{shock}\right) \quad (9)$$

$$\Delta p_{entry}^{non-shock} = -\frac{1}{2} \cdot \Delta p_{entry}^{shock} \quad (10)$$

$$\sum_{all\ arms} p_{entry} = 1 \quad (11)$$

The learning rate β used in Figure 1 was equal to 0.03.

Supplemental references

Bradski, G., 2000. The OpenCV Library. Dr. Dobb's J. Softw.

Burgess, H.A., Granato, M., 2007. Modulation of locomotor activity in larval zebrafish during light adaptation. J. Exp. Biol. 210, 2526–39. https://doi.org/10.1242/jeb.003939

Jolliffe, I., 2002. Principal Component Analysis, Springer Series in Statistics. Springer-Verlag, New York. https://doi.org/10.1007/b98835

Kalman, R.E., 1960. A New Approach to Linear Filtering and Prediction Problems. J. Basic Eng. 82, 35. https://doi.org/10.1115/1.3662552

Orger, M.B., Smear, M.C., Anstis, S.M., Baier, H., 2000. Perception of Fourier and non-Fourier motion by larval zebrafish. Nat. Neurosci. 3, 1128–1133. https://doi.org/10.1038/80649

Parks, T., McClellan, J., 1972. Chebyshev Approximation for Nonrecursive Digital Filters with Linear Phase. IEEE Trans. Circuit Theory 19, 189–194. https://doi.org/10.1109/TCT.1972.1083419

Ward, J.H., 1963. Hierarchical Grouping to Optimize an Objective Function. J. Am. Stat. Assoc. 58, 236. https://doi.org/10.2307/2282967